

Field-induced neutral Fermi surface and QCD₃-Chern-Simons quantum criticalities in Kitaev materials

LiuJun Zou^{1,2} and Yin-Chen He³

¹*Department of Physics, Harvard University, Cambridge, MA 02138, USA*

²*Department of Physics, Massachusetts Institute of Technology, Cambridge, MA 02139, USA*

³*Perimeter Institute for Theoretical Physics, Waterloo, Ontario N2L 2Y5, Canada*

We perform both numerical and theoretical studies on the phase diagram of the Kitaev materials in the presence of a magnetic field. We find that a new quantum spin liquid state with neutral Fermi surfaces emerges at intermediate field strengths, between the regimes for the non-Abelian chiral spin liquid state and for the trivial polarized state. We discuss the exotic field-induced quantum phase transitions from this new state with neutral Fermi surfaces to its nearby phases. We also theoretically study the field-induced quantum phase transitions from the non-Abelian chiral spin liquid to the symmetry-broken zigzag phase and to the trivial polarized state. Utilizing the recently developed dualities of gauge theories, we find these transitions can be described by critical bosons or gapless fermions coupled to emergent non-Abelian gauge fields, and the critical theories are of the type of a QCD₃-Chern-Simons theory. We propose that all these exotic quantum phase transitions can potentially be direct and continuous in the Kitaev materials, and we present sound evidence for this proposal. Therefore, besides being systems with intriguing quantum magnetism, Kitaev materials may also serve as table-top experimental platforms to study the interesting dynamics of emergent strongly interacting quarks and gluons in $2 + 1$ dimensions. Finally, we address the experimental signatures of these phenomena.

Contents

I. Introduction	1
II. Symmetries of the materials and models	3
III. Field-induced neutral Fermi surface	4
A. Numerical results	4
B. Parton theory of the NFS state	6
1. Transition into the trivial polarized state	7
2. Transition into ITO	8
IV. QCD ₃ -Chern-Simons quantum criticalities	9
A. Topological aspects and bosonic critical theories	9
B. Symmetry properties and dual fermionic theories	11
V. Discussion	13
VI. Acknowledgement	14
References	14
A. Symmetry actions of the Kitaev model and the neutral Fermi surface state	18
B. Kitaev model in terms of $SU(2)$ partons	19
C. Derivation of duality of critical theories	20
D. Parton mean field of the fermionic $U(2)$ critical theory	21

I. Introduction

Exploring exotic quantum phases and phase transitions is one of the frontiers of physics. Traditionally, quantum phases of matter are often distinguished by different patterns of spontaneous symmetry-breaking, and the low-energy excitations in these phases can be understood as long-lived quasi-particles. In the traditional wisdom, quantum phase transitions are often characterized by fluctuating order parameters of certain symmetries [1, 2].

Over the last decades, exotic quantum phases and phase transitions beyond the conventional paradigm are uncovered. The most well established examples may be the fractional quantum Hall (FQH) states, which are nontrivial phases of matter not associated with spontaneous symmetry-breaking. The low-energy excitations in the FQH states are still long-lived quasi-particles, but these quasi-particles are fractionalized, *i.e.*, they can carry fractional statistics and fractional charge [1].

Another class of long-sought exotic phases are quantum spin liquids (QSLs) [1]. A QSL is a spin system with a nontrivial structure of long-range entanglement in the ground state. QSLs can be broadly classified into two groups: gapped QSLs and gapless QSLs. A gapped QSL has an energy gap that separates its ground state(s) from its excited states, and its low-energy excitations also contain fractionalized long-lived quasi-particles, just as in the FQH states. In a gapless QSL, the dynamics is more complex because the excitations are gapless, and it may not be possible to view these excitations as any type of well-defined quasi-particles.

Despite the great progress in understanding QSLs

conceptually and the tremendous effort in searching them experimentally, so far no solid-state material has been unambiguously identified as a QSL. There are two main difficulties in finding a QSL experimentally: it often requires strong and certain particular form of interactions in the system to stabilize a QSL, and it is often difficult to find a smoking-gun signature to decide whether a system is a QSL. Because of these difficulties, it is of vital importance to build and realize realistic models that give rise to a QSL, and to develop effective methods to detect it.

One particularly interesting model of QSLs was proposed by Kitaev [3]. This is a model of localized spin-1/2 particles on a honeycomb lattice, and it features a rather special form of spin-spin interactions. By tuning the parameters in this model, Kitaev showed that this model can realize at least three different types of QSLs: a gapless QSL, a gapped Abelian QSL, and a gapped non-Abelian QSL. These gapped QSLs, if realized, are potentially useful in performing topological quantum computation [4].

The gapped non-Abelian QSL, more precisely speaking, realizes an Ising topological order (ITO), which has two types of fractionalized excitations: a non-Abelian anyon σ and a Majorana fermion. This state can be viewed as a $p+ip$ superconductor where the Bogoliubov quasi-particles therein are coupled to a dynamical Z_2 gauge field, and σ plays the role of the π flux in this superconductor. Just as a $p+ip$ superconductor, the ITO must break time reversal and mirror symmetries. In fact, it has a chiral edge mode of Majorana fermions, and it is supposed to have a quantized thermal Hall conductance $\kappa_{xy} = 1/2$ in units of $(\pi/6)(k_B^2 T/h)$. This property offers an experimentally feasible method to detect the ITO.

Because of the peculiar form of the spin-spin interaction in Kitaev's model, it seems rather unrealistic to be realized in a material. Remarkably, however, it was shown that some Mott insulators with strong spin-orbit coupling can potentially realize some variants of this model [5–7]. Since then, searching for Kitaev spin liquids in these materials becomes an active area. For recent reviews, see Refs. [8–10].

Among the various Kitaev materials, α -RuCl₃ has received significant attention recently. It is found that the ground state of α -RuCl₃ is magnetically ordered in the absence of a Zeeman field [11, 12]. Specifically, the spins are ordered in a zigzag pattern [13–15], as shown in Fig. 1. The Heisenberg and Γ interactions (introduced in Eq. (1)) are believed to be responsible for the zigzag order [16, 17], although the signs and strengths of these interactions in the real material are not fully settled down. It is also suggested that the Γ term may help to stabilize a QSL [18]. Notice a similar zigzag order has also been found in another Kitaev material, Na₂IrO₃ [19–21].

Upon applying a Zeeman field, the zigzag magnetic order in α -RuCl₃ melts [22–25]. If the Zeeman field

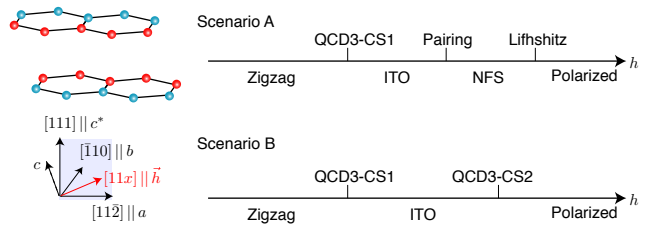


FIG. 1. Under a Zeeman field, a Kitaev material may go through four different phases (scenario A): a zigzag ordered state, a non-Abelian chiral quantum spin liquid with Ising topological order (ITO), a neutral Fermi surface (NFS) coupled to an emergent dynamical $U(1)$ gauge field, and a trivially polarized state. The phase transitions between these phases are described by the 1) QCD₃-Chern-Simons theory, 2) gauged pairing transition, and 3) gauged Lifshitz transition. Depending on the microscopic details (*e.g.*, direction and strength of the Zeeman field), there can also be a direct continuous quantum phase transition between the ITO state and the trivial polarized state, and the critical theory is described by another QCD₃-Chern-Simons theory (scenario B). The QCD₃-Chern-Simons transitions require a high symmetry of the system to be stable, which can be satisfied if the magnetic field is in the ac^* plane. All other phases and transitions do not rely on the high symmetries of the system.

is strong enough, the system will become a trivial polarized state. Remarkably, the measured thermal Hall conductance in certain range of field strengths is quantized exactly at the value predicted for the ITO [26], and this phenomenon is similar to that in the pure Kitaev model under a Zeeman field. Although there is some subtlety in interpreting this experiment [27–29], and the results therein need to be confirmed by further studies, this discovery has triggered great excitement.

These results give hope that α -RuCl₃ and other Kitaev materials may realize an ITO under a Zeeman field. Two interesting questions immediately arise:

- 1) By increasing the field, is the transition from the ITO to the trivially polarized state direct, or is there an intermediate phase?
- 2) Is there a theory that describes the quantum phase transition from the ITO to the magnetic order (*e.g.*, zigzag) upon decreasing the field?

We will address these two questions in this paper, and our main results are summarized in Fig. 1. Most surprisingly, we find that another QSL with a neutral Fermi surface (NFS) appears between the ITO and the trivially polarized state, as also suggested by Refs. [30–32]. This phase is described by a dynamical $U(1)$ gauge field coupled to Fermi pockets of fermionic spinons around Γ and $\pm K$ points of the Brillouin zone (BZ). Notice this dynamical $U(1)$ gauge field is emergent due to the nontrivial entanglement pattern of this state, and it should not be confused with the ordinary electromagnetic gauge field. The spinons, emer-

gent fermionic excitations, are neutral under the ordinary electromagnetic gauge field but interact strongly with the emergent dynamical $U(1)$ gauge field. Initially motivated by the physics of cuprate high-temperature superconductors [33], this state has been studied extensively over the years [34–44]. It is a very interesting type of QSL: it is gapless and its low-energy excitations cannot be viewed as well-defined quasi-particles, however, it is believed to be stable under any local perturbations, even if there is no symmetry to protect it. This property is very special, because usually a gapless state is stable if it is protected by some symmetry or all its excitations can be viewed as well-defined quasi-particles. We note that another material that also potentially realizes this state is the organic compound, κ -(BEDT-TTF) $_2$ Cu $_2$ (CN) $_3$ [45]. Recently, it was argued that YbMgGaO $_4$ also realizes this state [46], but this proposal is under debate [47].

The NFS state can serve as a mother state of the ITO state and the trivially polarized state. In particular, the ITO state can be obtained from the NFS state by pairing the spinons, and a critical theory for this transition has been discussed in Ref. [43]. The trivially polarized state can potentially be obtained from the NFS state by shrinking the Fermi pockets to zero size. This phase transition is a gauged Lifshitz transition, *i.e.*, a Lifshitz transition of fermions coupled to a dynamical $U(1)$ gauge field. Both these transitions are beyond the conventional paradigm because of the coupling to the dynamical gauge field. We will discuss the NFS state and these transitions both numerically and theoretically in Sec. III.

Another extremely intriguing aspect of this system is the possible exotic quantum phase transitions from the ITO state to the zigzag order and to the trivially polarized state, which can be realized by tuning the strength of the Zeeman field [26, 48]. We find that such quantum phase transitions are strikingly different from the conventional phase transitions, owing to the emergence of some deconfined non-Abelian gauge fields. In particular, these quantum critical points mimic the QCD theories in 2+1 dimensions, which have emergent quarks and gluons that are strongly interacting with each other. Moreover, these critical theories have interesting duality properties, namely, they can be described either by critical bosons interacting with a $U(2)$ Chern-Simons gauge field, or by gapless Dirac fermions interacting with a $U(2)$ Chern-Simons gauge field. Dualities of interacting gauge theories has generated huge theoretical enthusiasm in both the condensed matter and the high energy community [49–54], and the Kitaev materials may be one of the few experimental platforms [55] to study the duality proposals.

The rest of the paper is organized as follows. In Sec. II, we first review the global symmetries of some representative Kitaev materials, including α -RuCl $_3$, Na $_2$ IrO $_3$, etc. This will guide us to study different models in the later parts of the paper. In Sec. III, we

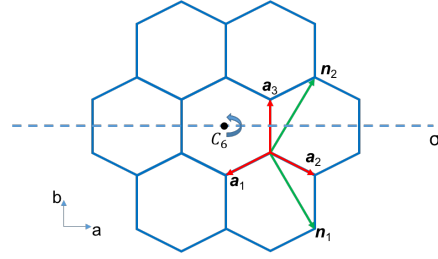


FIG. 2. The honeycomb lattice. The x -bond, y -bond and z -bond are along the direction of \mathbf{a}_1 , \mathbf{a}_2 and \mathbf{a}_3 , respectively. The a - and b -axes are shown in the figure, and the c^* -axis is perpendicular to the paper and pointing outwards.

first numerically study an idealized model, the Kitaev model under a magnetic field. We find strong evidence supporting the existence of the NFS state under an intermediate field. Then, through a parton construction, we provide theoretical understanding of this state and its transitions to the trivial polarized state and the ITO state. In Sec. IV, we discuss the quantum phase transitions from the ITO state to the zigzag phase and to the trivial polarized state, and we find they are described by emergent QCD $_3$ -Chern-Simons gauge theories. Finally, we summarize our results and discuss some future directions in Sec. V. The appendices contain various technical details.

II. Symmetries of the materials and models

A general Hamiltonian for a Kitaev material under a magnetic field up to nearest-neighbor coupling can be written as

$$H = \sum_{\langle ij \rangle \in \alpha} K_{\alpha} S_i^{\alpha} S_j^{\alpha} - \sum_i \mathbf{h} \cdot \mathbf{S}_i + J_H \sum_{\langle ij \rangle \in \alpha} \mathbf{S}_i \cdot \mathbf{S}_j + \sum_{\langle ij \rangle \in \alpha} \Gamma_{\alpha} S_i^{\beta} S_j^{\gamma}. \quad (1)$$

where the second and third terms are the familiar Zeeman field term and Heisenberg interaction, respectively. The $K_{\alpha} S_i^{\alpha} S_j^{\alpha}$ and $\Gamma_{\alpha} S_i^{\beta} S_j^{\gamma}$ terms are often referred to as the Kitaev term and Γ term, respectively. On the bond $\langle ij \rangle_x$, the x -bond connecting site i and site j , they denote terms $K_x S_i^x S_j^x$ and $\Gamma_x (S_i^y S_j^z + S_i^z S_j^y)$, respectively. And the similar notation is used for the y - and z -bonds. We denote the field direction $\mathbf{h} = (h_x, h_y, h_z)$ as $[h_x h_y h_z]$, and the field direction $\mathbf{h} = (-h_x, h_y, h_z)$ as $[\bar{h}_x h_y h_z]$.

This Hamiltonian is exactly solvable if only the Kitaev term is present. In this case, it hosts two spin liquid ground states. In particular, if $|K_x| < |K_y| + |K_z|$, etc., the ground state is a gapless Z_2 QSL with two Majorana cones. Under a small magnetic field, as shown by Kitaev, the Hamiltonian gives rise to an ITO, a non-Abelian chiral QSL ground state. Under a very large magnetic field, the spins are trivially polarized [3].

	$T_{1,2}$	C_2	\mathcal{T}	σ^*	$\mathcal{T}\sigma^*$
$\mathbf{h} = 0$	Yes	Yes	Yes	Yes	Yes
$\mathbf{h} \parallel [11x]$, in ac^* plane	Yes	Yes	No	No	Yes
$\mathbf{h} \parallel [\bar{1}10]$, parallel to b	Yes	Yes	No	Yes	No
$\mathbf{h} \nparallel [\bar{1}10], [11x]$	Yes	Yes	No	No	No

TABLE I. Symmetries of some representative Kitaev materials (including α -RuCl₃, Na₂IrO₃, etc.) under the Zeeman field along different field direction $\mathbf{h} = (h_x, h_y, h_z)$.

Once perturbed away from the pure Kitaev model, the Hamiltonian is no longer exactly solvable. It is still an open issue about the precise values of the coupling constants of each interaction term. In this paper, we will be primarily concerned with the symmetries of the system, and will not worry about the microscopic interaction strengths.

Some representative Kitaev materials, including α -RuCl₃, Na₂IrO₃, etc., are layered quasi-two-dimensional materials with point group symmetry C_2/m [10].¹ The C_2/m symmetry constrains that $K_x = K_y$, $\Gamma_x = \Gamma_y$. It is expected that $K_z \sim K_{x,y}$ and $\Gamma_z \sim \Gamma_{x,y}$, but it is not crucial for our discussion. Without the Zeeman field, the Hamiltonian enjoys the translation symmetry $T_{1,2}$ along $\mathbf{n}_{1,2}$, inversion symmetry C_2 , pseudo-mirror symmetry σ^* (with the mirror axis perpendicular to the z bond, or, equivalently, along the dashed line in Fig. 2), and time-reversal symmetry \mathcal{T} ($\mathbf{S} \rightarrow -\mathbf{S}$). The pseudo-mirror symmetry σ^* is the conventional mirror symmetry followed by a spin rotation symmetry $e^{i\pi S^y} e^{i\pi/2 S^z}$,

$$\sigma^* : S_{\mathbf{r}}^x \rightarrow -S_{\sigma\mathbf{r}}^y, \quad (2)$$

$$S_{\mathbf{r}}^y \rightarrow -S_{\sigma\mathbf{r}}^x, \quad (3)$$

$$S_{\mathbf{r}}^z \rightarrow -S_{\sigma\mathbf{r}}^z. \quad (4)$$

We remark that the spin flip symmetries $e^{i\pi S^\alpha}$ are broken due to the Γ terms.

Under a finite Zeeman field, the time reversal symmetry will be broken. The pseudo-mirror symmetry is also broken by a field along a generic direction. There are special directions along which the pseudo-mirror symmetry or its combination with the time-reversal symmetry is preserved. The details are summarized in Table I.

The time reversal symmetry \mathcal{T} or the pseudo-mirror symmetry σ^* forbids a finite thermal Hall conductance. Therefore, if the Zeeman field is parallel to the b axis

($[\bar{1}10]$ direction), one cannot have a ITO unless σ^* is spontaneously breaking. On the other hand, if the Zeeman field is on the ac^* plane, as is done in the thermal Hall experiments [26], there is no symmetry that forbids the ITO. However, it does not mean that we should expect an ITO for a field in a generic direction on the ac^* plane. After all, if one rotates the field on the ac^* plane, there should be a phase transition between the ITO and its time-reversal partner. This transition can be direct and continuous, or there can be an intermediate phase, *e.g.*, a Z_2 toric code phase, as one rotates the Zeeman field on the ac^* plane. In this paper, we will not pursue in this direction.

Interestingly, the combination of time-reversal and pseudo-mirror symmetry, $\mathcal{T}\sigma^*$, is preserved for the field on the ac^* plane ($\mathbf{h} \parallel [11x]$). This symmetry is crucial for the stability of the QCD₃-Chern-Simons quantum critical points, as we will discuss in Sec. IV. The NFS, on the other hand, is not sensible to any symmetry breaking perturbation. We note that Refs. [15, 58] reported that the zigzag order is on the ac^* plane, which means this order preserves σ^* and breaks $\mathcal{T}\sigma^*$.

III. Field-induced neutral Fermi surface

To discuss the main features of the NFS state, we consider an idealized model, *i.e.*, an isotropic Kitaev model ($K_x = K_y = K_z = K$) under a Zeeman field along the $[111]$ direction $\mathbf{h} = h(1, 1, 1)$. Meanwhile, we neglect the Γ and Heisenberg interactions. For this special choice of parameters, the system has an extra symmetry, namely, $C_6^* = C_6 \cdot e^{i2\pi/3(S_x + S_y + S_z)/\sqrt{3}}$. Since the NFS is rather insensitive to various perturbations, the main features in this ideal model will still hold after including other realistic interactions and symmetry breaking effects in materials. However, a higher symmetry puts more constraints on the microscopic theory of the gapless spin liquid, and yields more clear predictions that can be tested numerically.

A. Numerical results

We use the infinite DMRG algorithm [59–61] to simulate the Hamiltonian Eq. (1) with $K_x = K_y = K_z = 1$, $h_x = h_y = h_z = h$, and $\Gamma = J = 0$. There is previous numerical work studying similar Hamiltonians [30–32, 62]. We wrap the honeycomb lattice on a cylinder (as shown in the Fig. 3a). There are L_y unit cells around the cylinder (\mathbf{e}_1 direction), and an infinite number of unit cells along the cylinder (\mathbf{e}_2 direction). Due to the lack of any conserved quantum number in the Hamiltonian, the simulation is more expensive compared to the familiar spin models (*e.g.*, the Heisenberg model). We carry out simulations for two different sizes, $L_y = 2, 3$ unit cells (*i.e.*, $L_y = 4, 6$ sites), and we keep the bond dimension of DMRG up to

¹ We note that there is debate on the precise symmetry of α -RuCl₃. Some recent papers claim the symmetry is C_2/m [14, 15], while some others claim the symmetry should be $R\bar{3}$ [56, 57]. Here we assume the symmetry is C_2/m , and the general method presented in this paper can also be straightforwardly adapted to other symmetry settings.

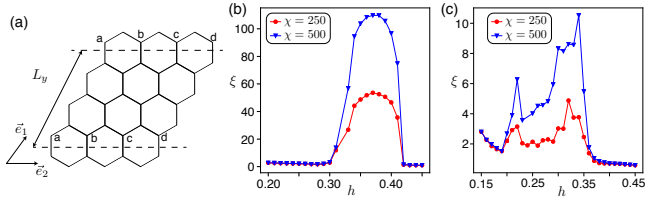


FIG. 3. (a) Cylinder geometry used in DMRG simulations. Here we plot an example with $L_y = 3$ unit cells (6 sites). The sites labeled by the same letters are identified. (b), (c) The dependence of the correlation length ξ on the magnetic field strength h and bond dimension χ on the (b) $L_y = 2$ cylinder and the (c) $L_y = 3$ cylinder.

$\chi \approx 1400 \sim 2000$. The truncation error is reasonably small, $\sim 10^{-10}$ for $L_y = 2$ unit cells and $\sim 10^{-7}$ for $L_y = 3$ unit cells, signifying the convergence of DMRG simulations.

Fig. 3(b)-(c) show the behavior of correlation length ξ (along \mathbf{e}_2) as the magnetic field h changes. Clearly the correlation length is pretty large in a finite region of intermediate field strengths, $h \in (0.31, 0.41)$ for $L_y = 2$ unit cells and $h \in (0.24, 0.36)$ for $L_y = 3$ unit cells. Moreover, the correlation length ξ increases significantly with the bond dimension χ , which is typical for a gapless state in the infinite DMRG simulation. In contrast, in the smaller field (gapped ITO) or larger field region (polarized state), the correlation length does not show any dependence on the bond dimension. This simple observation provides convincing evidence for the existence of a gapless phase in the region of intermediate field strengths. The gapless state is supposed to have a divergent correlation length in the 2D limit, but in the simulations the finite bond dimension χ introduces a cutoff. Meanwhile, for a given bond dimension, the system with a larger size gets a larger truncation, hence the cylinder with $L_y = 3$ has a smaller correlation length than the one with $L_y = 2$ with the same bond dimension. We think it is the finite size effect that makes the parameter regimes for this gapless phase different on the cylinders with $L_y = 2$ and $L_y = 3$. In the following, we will show that this gapless phase is consistent with an NFS phase, *i.e.*, Fermi surfaces coupled to a $U(1)$ gauge field. For numerical studies on the gapped ITO, we refer the readers to Refs. [30–32].

On a cylinder, the momenta k_1 (along \mathbf{e}_1) are quantized with a spacing $2\pi/L_y$ due to the finite L_y . Therefore, instead of having a genuine 2D state in our system, we expect a number of 1D wires of fermionic spinons labeled by k_1 , as shown in Fig. 4(a)-(b). In the 2D limit, the spinons are forming Fermi surfaces around high symmetry points. On the cylinder, these Fermi surfaces would then be cut by the 1D wires (according to their momenta), yielding gapless modes. In the case of free fermions, the number of gapless modes are simply the number of cuts between the 1D wires

and Fermi surfaces. In our case, the fermionic spinons are interacting with a dynamical $U(1)$ gauge field. As shown in Ref. [63], the $U(1)$ gauge field will change the system into a set of coupled Luttinger liquids with central charge $c = N_w - 1$, where N_w is the central charge of the naive free fermion limit.

To extract the central charge of the gapless phase, we use the finite entanglement scaling introduced in Ref. [64]. As shown in the Fig. 4(c)-(d), the central charge is $c = 1$ on the $L_y = 2$ cylinder and is $c = 2$ on the $L_y = 3$ cylinder. This indicates that the 1D wires cut the Fermi surfaces twice on the $L_y = 2$ cylinder, and three times on the $L_y = 3$ cylinder. One consistent scenario is shown in Fig. 4(a)-(b). On the $L_y = 2$ cylinder, both the K and $-K$ Fermi pockets are cut once by the wires $k_1 = \pi/2$ and $k_1 = -\pi/2$ respectively. On the $L_y = 3$ cylinder, the Fermi pocket around the Γ point is cut once by the wire with $k_1 = 0$; while the Fermi pocket around the K ($-K$) point is cut once by the wires with $k_1 = 2\pi/3$ ($k_1 = -2\pi/3$). One may note that the quantized momenta on the $L_y = 2$ and $L_y = 3$ are corresponding to different boundary conditions of fermionic spinons. This is made possible by the fact that the spinons are interacting with a $U(1)$ gauge field. Consequently, a gauge flux ϕ can in principle be trapped in the cylinder [65, 66]. Moreover, due to the C_2 symmetry, ϕ should be quantized to either 0 or π . In other words, the fermionic spinons have either a periodic or an anti-periodic boundary condition, depending on the microscopic energetics.

Having established a field-induced NFS state in the Kitaev model, it is important to know which operators can detect the $2k_f$ scattering modes of the Fermi surfaces. We calculate the static structure factor of spin operators,

$$D_{xx}(q_1, q_2) = \sum_r e^{-iq_1 r_1 - iq_2 r_2} S_0^x S_r^x. \quad (5)$$

where $q_{1,2}$ and $r_{1,2}$ are the components of \mathbf{q} and \mathbf{r} along $\mathbf{e}_{1,2}$, respectively. Fig. 5 shows $|D_{xx}(q_1, q_2 = 0)|$ on the $L_y = 3$ cylinder, which clearly has singular peaks at the finite momenta $q_2 = \pm 2k_f$. By detailed examination of the spectra of correlation lengths [66, 67], we conclude these singular peaks correspond to a $2k_f$ scattering mode from the Fermi pockets around the $\pm K$ points. Ideally, there are other scattering modes, such as the $2k_f$ modes at the Γ pocket as well as the scattering modes between the $\pm K$ pockets and the Γ pocket. However, they do not have any sharp features in our numerical data of static structure factor. We think this is due to the possibility that those modes have a much smaller correlation length, hence their signatures are washed out.

Therefore, correlation functions of the single spin operator S^α can detect the gapless modes of the NFS state. It is in sharp contrast to the Z_2 gapless Majorana cone state in the isotropic Kitaev model, in which the simple spin excitation is gapped due to the gapped

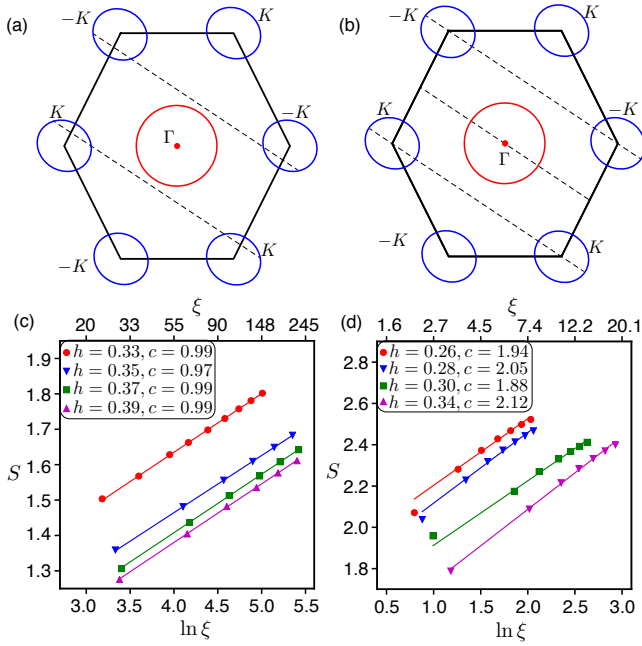


FIG. 4. (a), (b): Schematic illustration of Brillouin zone (BZ) and Fermi pockets. The dashed line represent the momenta points accessible on (a) the $L_y = 2$ cylinder and (b) the $L_y = 3$ cylinder. The spinons have anti-periodic boundary condition on the $L_y = 2$ cylinder, and periodic boundary condition on the $L_y = 3$ cylinder. (c), (d): Central charge fitting for the (c) $L_y = 2$ cylinder and (d) $L_y = 3$ cylinder.

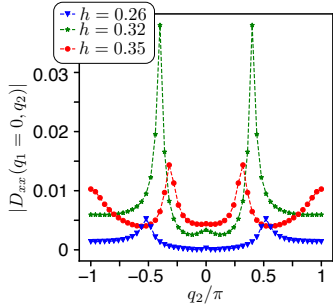


FIG. 5. The static structure factor of S^x on the $L_y = 3$ cylinder. The value of $2k_f$ decreases as the field strength increases, which is a signal that the NFS shrinks as the field increases.

visions [68]. We expect that experimental techniques such as neutron scattering is able to directly measure the Fermi surfaces of spinons.

Our numerical data could also be consistent with a scenario with only one Fermi pocket around the Γ point. However, such a state at the mean field level will violate the Luttinger volume law, for which we are not able to find a theory. On the other hand, theoretically we could also imagine there are Fermi pockets only around $\pm K$ points, or around both the $\pm K$ and $M_{1,2,3}$ points. However, these are not consistent with

numerical results. In the former case, for example, one would always expect an odd central charge, which contradicts with $c = 2$ we obtained on the $L_y = 3$ cylinder.

At last, we remark that, if the size of the $\pm K$ pockets are large, the $k_1 = \pm\pi/2$ wires on the $L_y = 2$ cylinder may also cut through them. If this happens, we expect a larger central charge, for example $c = 3$. Similar scenario could happen for the $L_y = 3$ cylinder, where the $k_1 = \pm 2\pi/3$ wires could also cut the Γ pocket if the latter is large enough. However, we have not observed this in our numerical simulations.

Below we turn to understanding our numerical results theoretically.

B. Parton theory of the NFS state

From Kitaev's original analysis, it is known that the isotropic Kitaev model perturbed by a weak magnetic field hosts a non-Abelian ITO [3]. In Sec. III A, we have demonstrated that a different QSL state that has a NFS can be stabilized when the magnetic field becomes stronger. This state persists in a range of magnetic fields, and finally becomes a trivial polarized state. These phenomena can be understood in the following picture.

Previous studies indicate that an NFS state can become an ITO through a continuous quantum phase transition by condensing Cooper pairs of fermionic spinons [43], which is a natural scenario in our system when the magnetic field is decreased so that the NFS state transits into the ITO. On the other hand, when the magnetic field is increased, the Fermi surface of the NFS state may shrink and disappear. Then the gauge fluctuations will render the system a short-range entangled state [69], which can be the trivial polarized state. To gain more insights, in this subsection we provide a parton mean field theory for the NFS state and its transitions out. Note to get the the full theory beyond the mean field, one must incorporate the coupling between the spinons and the dynamical $U(1)$ gauge field.

Before presenting our parton mean field theory, let us pause for a moment to explain two principles to find such a theory. First, because we would like to have both the NFS and ITO states preserve translation, C_6^* and $\mathcal{T}\sigma^*$ symmetries, and to have a scenario that condensing spinon pairs in the NFS state leads to the ITO state, all symmetries of the ITO mean field must also be present in the NFS mean field. Second, we would like to have a parameter regime in which there are Fermi pockets around Γ , K and $-K$ points of the BZ, respectively.

We will use the standard $SU(2)$ parton construction, which writes the spin operator in terms of fermionic spinon operators [1, 70]:

$$\mathbf{S}_i = \frac{1}{2} f_i^\dagger \boldsymbol{\sigma} f_i \quad (6)$$

where \mathbf{S}_i represents the spin operator at site i , $f_i = (f_{i1}, f_{i2})^T$ is a two-component fermionic spinon operator, and σ denotes the usual Pauli matrices. The physical states in the Hilbert space satisfy the constraint

$$f_i^\dagger f_i = 1 \quad (7)$$

This parton construction has an $SU(2)$ gauge structure [1, 70], but for our purpose the $SU(2)$ gauge structure will be broken down to $U(1)$, where the gauge transformation reads $f_i \rightarrow f_i e^{i\theta_i}$. We will use the terminology that f_i carries gauge charge 1. Notice this is the charge under an emergent dynamical $U(1)$ gauge field, which should not be confused with the ordinary $U(1)$ electromagnetic field. In fact, these spinons are neutral under the usual electromagnetic field.

This formalism has been applied to study the Kitaev model [71, 72]. In particular, the implementation of symmetries in the Kitaev model is discussed in Ref. [72], where it is shown that f becomes a linear combination of f and f^\dagger under the relevant symmetry transformations, *i.e.*, the symmetry transformations mix positive and negative gauge charges. This type of symmetry actions is unnatural to describe a $U(1)$ quantum spin liquid with an NFS, where a more natural symmetry implementation should either preserve the gauge charge (*i.e.*, take f to f) or flip the gauge charge (*i.e.*, take f to f^\dagger). If the symmetries flip the gauge charge, it would mean that whenever there is a Fermi pocket around the Γ point, there needs to be a hole pocket around the Γ point as well. Similarly, there will also be two pockets around K and $-K$ with opposite gauge charges. This leads to more than three pockets in the BZ, which is inconsistent with our numerical results that indicate there are only three pockets, around Γ , K and $-K$, respectively. Therefore, we will look for a symmetry implementation that preserves the gauge charge of the spinons.

Although the gauge charges are mixed under the symmetry actions in the $SU(2)$ parton formulation described in Ref. [72], these symmetry actions themselves can be changed by utilizing the gauge freedom in the parton construction (6). In particular, in Appendix A we present a gauge transformation under which the symmetry actions of the Kitaev model become those in Table II, where we can see explicitly that the gauge charge is preserved under the symmetry actions.

	$T_{1,2}$	C_6^*	$\mathcal{T}\sigma^*$
$f(\mathbf{r}_i) \rightarrow$	$f(\mathbf{r}_i + \mathbf{n}_{1,2})$	$e^{i\frac{5\pi}{6}} \sigma_{C_6^*}^\dagger f(C_6 \mathbf{r}_i)$	$e^{-i\frac{\pi}{4}} \sigma_{\mathcal{T}\sigma^*}^\dagger f(\sigma \mathbf{r}_i)$

TABLE II. Symmetry actions on the spinons. Adopting the notations in Ref. [72], $\sigma_{C_6^*} \equiv \frac{1+i(\sigma_1+\sigma_2+\sigma_3)}{2}$ and $\sigma_{\mathcal{T}\sigma^*} \equiv e^{-i\sigma_3 \frac{\pi}{4}}$. Notice multiplying these transformation rules by a $U(1)$ phase factor gives rise to the same physical symmetry action in the NFS state, because this does not change the symmetry action on any physical (gauge invariant) operator.

After performing this gauge transformation, the Kitaev model rewritten in terms of the spinon operators f contains two types of terms:

$$H_K = H_{\text{hopping}} + H_{\text{pairing}} \quad (8)$$

The detailed form of these terms are given in Appendix B, and here we only note that H_{hopping} contains only hopping operators of the spinons, *i.e.*, each term in H_{hopping} preserves the $U(1)$ gauge charge of the spinon. On the other hand, H_{pairing} contains purely pairing of the spinons, *i.e.*, each term in H_{pairing} breaks the $U(1)$ gauge structure to a Z_2 gauge structure. Furthermore, both H_{hopping} and H_{pairing} preserve the symmetries in Table II.

The mean field Hamiltonian that we will construct for the NFS state is given by

$$H_{\text{NFS}} = H_{\text{hopping}} + H_h \quad (9)$$

where

$$H_h = -h \sum_i f_i^\dagger (\sigma_1 + \sigma_2 + \sigma_3) f_i \quad (10)$$

represents the Zeeman coupling to a magnetic field in the (111) direction.² This Hamiltonian also preserves all symmetries in Table II.

The representative dispersions of this four-band mean field Hamiltonian are shown in Fig. 6. As we can see, for a range of magnetic fields, an NFS state is realized, where the chemical potential cuts through the second and the third bands (in the first three figures of Fig. 6). Furthermore, there are in total three Fermi pockets that are around Γ and $\pm K$, respectively. The Fermi pockets around K and $-K$ carry the same gauge charge, which is consistent with the C_6^* and $\mathcal{T}\sigma^*$ symmetries. The Fermi pocket around Γ carries opposite gauge charge compared to the two at $\pm K$, which is consistent with the Luttinger theorem applied to the mean field Hamiltonian (9) subject to the constraint $\langle f_i^\dagger f_i \rangle = 1$. We note that our state is different from the spinon-Fermi-surface state in Ref. [73], where the spinons are coupled to a dynamical Z_2 gauge field.

The NFS state with gauge fluctuations taken into account is still a stable quantum phase of matter, and its properties have been studied extensively [36, 39–44]. Below we discuss the quantum phase transitions from the NFS state to the trivial polarized state and to the ITO state.

1. Transition into the trivial polarized state

Upon increasing the magnetic field, the pockets change in size and shape, and eventually disappear.

² We note that H_h should not be literally taken as the full effect of a Zeeman field, because a Zeeman field can also renormalize the parameters in other terms of the Hamiltonian.

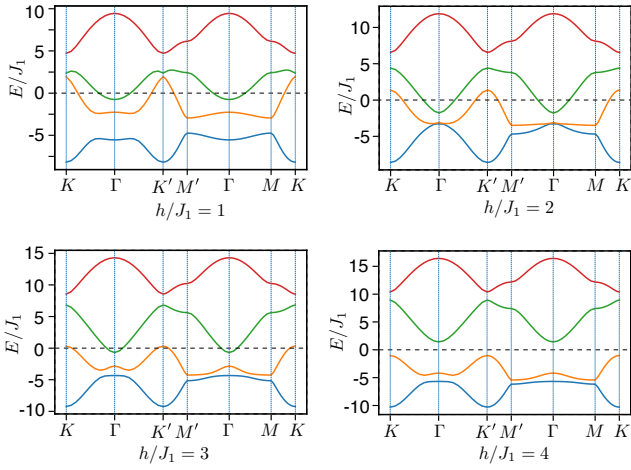


FIG. 6. Representative dispersions of the Hamiltonian (9). The parameters we use are $J'_1/J_1 = 3.75$, $J_2/J_1 = -0.75$, and $h/J_1 = 1, 2, 3, 4$ for the four dispersions, respectively. The definitions of the parameters J_1 , J_2 and J'_1 are given in Appendix B. In all these dispersions, the chemical potential is tuned so that the gauge constraint (7) is satisfied at the level of expectation values: $\langle f_i^\dagger f_i \rangle = 1$.

We note in this process there can be Dirac crossings of the four bands, but such Dirac crossings are found to always occur away from the chemical potential, so they do not induce a phase transition. When the magnetic field exceeds some critical value where the pockets disappear, the dynamical $U(1)$ gauge field will be confined due to the proliferation of monopoles [69]. The precise nature of the confining state will depend on the quantum numbers of the monopole, which in turn depends on the mean field Hamiltonian of the spinons. In this regime where the pockets disappear upon increasing the field, the two lower filled bands can be smoothly deformed into a trivial atomic limit on the honeycomb lattice with $h \rightarrow \infty$. Following the argument in Ref. [74], this means the quantum numbers of the monopole are trivial, and the resulting state after the proliferation of monopoles is consistent with a trivial symmetry-preserving short-range entangled state, *i.e.*, the trivial polarized state.

Notice that as the Fermi volume decreases, there can potentially be other instabilities (towards, *e.g.*, exciton condensation). In this case, there will be an intermediate state between the NFS state and the trivial polarized state.

Therefore, our theory is potentially capable of describing the quantum phase transition from the NFS state to the trivial polarized state by increasing the magnetic field. The putative critical theory for this transition is a gauged Lifshitz transition, where fermions coupled to a dynamical $U(1)$ gauge field are undergoing a Lifshitz transition. We conjecture that the confining state is indeed the polarized state, and this transition can indeed be continuous. More detailed

studies of this phase transition are left to the future.

2. Transition into ITO

Now we turn to the transition from NFS to ITO. A usual Fermi liquid is unstable to an infinitesimal attractive interaction, which will induce pairing. According to Ref. [43], however, the gauge fluctuations make an NFS state stable against an infinitesimal attractive interaction among the spinons, and only if this attractive interaction is stronger than a critical value does the NFS state undergo a pairing transition. In our case, the strength of the attractive interaction among the spinons depends on the microscopic details, such as the external magnetic field. It is natural to expect that, at a certain Zeeman field, the attractive interaction becomes critical and the pairing transition takes place.

To gain more insight into this transition, consider adding a pairing term so that the Hamiltonian becomes

$$H = H_{\text{NFS}} + \lambda_{\Delta} H_{\text{pairing}} \quad (11)$$

where $\lambda_{\Delta} \in [0, 1]$. This pairing term is supposed to be induced by some attractive interaction among the spinons.

We check the effect of the pairing term numerically. For concreteness, let us focus on the case where $h = J_1$ (panel (a) in Fig. 6). We find that an infinitesimal λ_{Δ} is able to open a gap for the Hamiltonian Eq. (11). After this gap is opened, we calculate the Chern number of the ground state using the method in Ref. [75], and find a Chern number consistent with that of a $p \pm ip$ superconductor.³ This means by this pairing transition our NFS state can become an ITO, and this phase transition can be a generic second-order transition according to Ref. [43].

We caution the reader that so far we have only shown that after the above pairing transition, the NFS state becomes a non-Abelian ITO, but we have not proved that this ITO is identical to that of the Kitaev model. This is because the mean field state described by Eq. (11) may differ from Eq. (8) by a symmetry-protected topological (SPT) state under the symmetries in Table II, which, after taking into account the coupling between the spinons and gauge field, can potentially lead to a symmetry-enriched topological (SET) state that is distinct from the one described by the Kitaev model.⁴

³ We note that, in the discussion of this type of mean field theory, the difference between $p + ip$ and $p - ip$ superconductors is inessential, because one can always apply a parity transformation to the Hamiltonian (11) to convert one of them into the other, in a way that the Zeeman field term (10) is invariant.

⁴ We note there are also examples of distinct phases that become identical when coupled to a dynamical gauge field. For example, see [76–79].

To settle down this potential ambiguity, we design an interpolating family of Hamiltonians that connect Eq. (11) and Eq. (8). More precisely, consider the Hamiltonian family parameterized by λ_Δ and λ_h :

$$H(\lambda_\Delta, \lambda_B) = H_{\text{hopping}} + \lambda_h H_h + \lambda_\Delta H_{\text{pairing}} \quad (12)$$

Clearly, $H(\lambda_\Delta, 1)$ gives Eq. (11), and $H(1, 0)$ gives Eq. (8). Also, notice this entire family of Hamiltonians respect the symmetries in Table II. To connect (11) to (8), we first increase λ_Δ from 0 to 1 while fixing $\lambda_h = 1$. After this is done, we decrease λ_h from 1 to 0 while fixing $\lambda_\Delta = 1$. We find that, apart from the initial point with $(\lambda_\Delta, \lambda_h) = (0, 1)$, an energy gap is always finite in the entire interpolation, which establishes that Eq. (11) and Eq. (8) indeed describe the same quantum phase. Therefore, by condensing pairs of spinons our NFS state can indeed transit into the Kitaev spin liquid.

IV. QCD₃-Chern-Simons quantum criticalities

In the previous section, we have discussed the quantum phase transition between the NFS state and the polarized state, as well as the transition between the NFS state and the ITO state. Both transitions are beyond the conventional paradigm. In this section, we study the possible exotic quantum phase transitions from the ITO state to the zigzag phase and to the polarized phase. These two states have no topological order, so these transitions can be viewed as confinement transitions of the ITO.

At a first glance, such confinement transitions are rather nontrivial if they can be continuous. To appreciate this, first notice the anyonic excitations in the ITO only include the non-Abelian Ising anyon σ and the Majorana fermion. One common way to confine a topological order is to condense some of its anyonic excitations that have bosonic self-statistics and proper mutual statistics with other anyons. In ITO, however, there is no obvious such (bosonic) anyon that can condense. One may also try to describe the transition in terms of gapless fermions coupled to gauge fields. As mentioned in the introduction, the ITO can be understood as a Z_2 gauge field coupled to Majorana fermions in a topological band with Chern number $C = 1$. To confine the ITO, one needs to first change the Chern number of the Majorana fermions from $C = 1$ to $C = 0$. This process yields a pure deconfined Z_2 gauge theory, which is the more familiar Z_2 toric code state [3]. To get a topologically trivial state, one needs to further confine the pure Z_2 gauge theory. In other words, one needs two separate transitions to confine the ITO. The first transition is described by a single Majorana cone coupled to a Z_2 gauge field, and the second transition is the confinement transition of the pure Z_2 gauge theory, which can be described by an Ising order parameter

coupled to a Z_2 gauge field [80].⁵

The way to make progress, as we will discuss in the following, is to consider dual topological quantum field theory (TQFT) descriptions of the ITO. More precisely, we will find other gauge theories that are capable of describing the ITO, such that the confinement transitions of these gauge theories can be understood either by critical bosons or gapless fermions coupled to the gauge fields.

A. Topological aspects and bosonic critical theories

To apply this strategy to our case, first recall that the ITO can be viewed as a $p + ip$ superconductor coupled to a dynamical Z_2 gauge field that corresponds to the fermion parity symmetry, *i.e.*, the ITO is a gauged $p + ip$ superconductor. Furthermore, there is a 16-fold-way classification of $2 + 1$ D gapped superconductors coupled to such a Z_2 gauge field, where the ITO corresponds to the state with an index $\nu = 1$ [3]. Suppose we take the superconductor with $\nu = 3$ together with another superconductor with $\nu = -2$, and weakly hybridize the fermions in these two superconductors, the resulting state is the one with $\nu = 1$.

This observation is useful because it is known that the state with $\nu = 3$ can be described by an $SU(2)_2$ Chern-Simons theory coupled to a boson. This theory also has two nontrivial anyons: a non-Abelian anyon σ' and a Majorana fermion. In addition, the state with $\nu = -2$ can be described by a $U(1)_{-4}$ Chern-Simons theory coupled to a boson, and this theory has three nontrivial Abelian anyons, with one of them a Majorana fermion. Therefore, we can arrive at the ITO state by taking an $SU(2)_2$ theory and a $U(1)_{-4}$ theory, and hybridizing the Majorana fermions in these two theories. More formally, this hybridization of the Majorana fermions can be viewed as a process of anyon condensation, where the bound state of the Majorana fermions from the $SU(2)_2$ and $U(1)_{-4}$ theories are condensed. In the language of TQFT, the resulting coupled theory is denoted as $U(2)_{2,-2}$,⁶ and we have derived a known duality [81]

$$\text{Ising TQFT} \longleftrightarrow U(2)_{2,-2} = \frac{SU(2)_2 \times U(1)_{-4}}{\mathbb{Z}_2}. \quad (13)$$

The Lagrangian of the $U(2)_{2,-2}$ theory can be writ-

⁵ We note that due to the coupling to a dynamical Z_2 gauge field, the first transition is in a distinct universality class compared to a single free gapless Majorana fermion, and the second transition is also in a distinct universality class compared to the 3D Ising transition.

⁶ In Ref. [54], this theory is denoted as $U(2)_{2,-2}$. In Ref. [81], it is denoted as $U(2)_{2,-4}$.

ten as

$$\mathcal{L}_{\text{CS}} = -\frac{2}{4\pi}\text{Tr}(\mathbf{b}d\mathbf{b} - \frac{2i}{3}\mathbf{b}^3) + \frac{2}{4\pi}(\text{Tr}\mathbf{b})d(\text{Tr}\mathbf{b}). \quad (14)$$

where $\mathbf{b} = b + \tilde{b}\mathbf{1}$ is a 2-by-2 $U(2)$ gauge field, with b an $SU(2)$ gauge field and \tilde{b} a $U(1)$ gauge field.⁷

This $U(2)$ gauge field is coupled to dynamical bosonic matter fields Φ , so that the total Lagrangian is

$$\mathcal{L} = \mathcal{L}_{[\Phi, \mathbf{b}]} + \mathcal{L}_{\text{CS}} + \mathcal{L}_{\text{Maxwell}} - \frac{1}{2\pi}Bd(\text{Tr}\mathbf{b}) + \dots \quad (15)$$

Here Φ may have different flavors, and each flavor can be thought of as a two-component (corresponding to the color index) complex boson, $\Phi = (\phi_a, \phi_b)^T$, which are in the fundamental representation of the $U(2)$ gauge group. The third term $\mathcal{L}_{\text{Maxwell}}$ is the standard Maxwell Lagrangian of the gauge field, and at long distances it is less relevant compared to the topological part, Eq. (14).

Before proceeding, we pause to comment on the global symmetries of the theory Eq. (15) in the absence of the last \dots term. As a quantum field theory in the continuum, besides the Poincare symmetry, CPT symmetry, etc., this theory also enjoys a $U(1)$ symmetry corresponding to the gauge flux conservation of \tilde{b} , as well as an $SU(N_f)$ flavor symmetry. These symmetries may not be present in the physical system, but it is nevertheless helpful to keep track of them. The microscopic symmetries of the physical system must be embedded into these symmetries, but, *a priori*, the precise embedding pattern can only be determined after we have a concrete microscopic construction where this field theory emerges at long distances. When specifying to the physical system, we will add appropriate \dots terms to Eq. (15) to break its full symmetries to the physical symmetries. For example, we can add monopole operators of \tilde{b} to break the $U(1)$ flux conservation symmetry, and add certain quartic interactions to break this $SU(N_f)$ flavor symmetry. To keep track of the $U(1)$ symmetry, we have added the fourth term, where B is the probe gauge field of this $U(1)$ symmetry.

The dynamics of the bosonic field Φ is described by the standard ϕ^4 theory, with $N_f = 1, 2$ flavors,

$$\mathcal{L}_{[\Phi, \mathbf{b}]} = \sum_{I=1}^{N_f} |(\partial_\mu - i\mathbf{b}_\mu)\Phi_I|^2 - m \sum_I |\Phi_I|^2 - V(\Phi). \quad (16)$$

where $V(\Phi)$ is the symmetry-consistent quartic potential term.

⁷ This theory can also be written as,

$$\mathcal{L}_{\text{CS}} = -\frac{2}{4\pi}\text{Tr}(bdb - \frac{2i}{3}b^3) + \frac{4}{4\pi}\tilde{b}d\tilde{b}.$$

If the Φ fields are gapped, they are dynamically trivial and hence can be simply neglected. The theory is then described by the $U(2)_{2,-2}$ theory, which is nothing but the ITO. On the other hand, if the Φ fields are condensed, the $U(2)$ gauge field will be Higgsed, which destroys the ITO. The mass of Φ is the tuning parameter for this phase transition. In the continuum field theory, it is straightforward to understand the phases when Φ is condensed.

When $N_f = 1$, the $U(2)$ gauge field is Higgsed down to $U(1)$. Without loss of generality, let us suppose the first color component of Φ gets a nonzero vacuum expectation value, then only b_{22} is an active gauge field. In the absence of the \dots term in Eq. (15), the Lagrangian describing this remaining gauge field is

$$\begin{aligned} \mathcal{L} &= -\frac{2}{4\pi}b_{22}db_{22} + \frac{2}{4\pi}b_{22}db_{22} + \mathcal{L}_{\text{Maxwell}} - \frac{1}{2\pi}Bdb_{22} \\ &= \mathcal{L}_{\text{Maxwell}} - \frac{1}{2\pi}Bdb_{22}. \end{aligned} \quad (17)$$

So we end up with a 2 + 1D $U(1)$ Maxwell theory, which is nothing but a Goldstone phase with the $U(1)$ flux conservation symmetry spontaneously broken [82]. In the Kitaev materials, this $U(1)$ symmetry should be explicitly broken, and the monopole operators responsible for this symmetry breaking will gap out the Goldstone mode. Physically, it may be tempting to identify this phase as the zigzag phase. However, the precise nature of this confined state depends on the quantum numbers of the monopoles, which we will discuss in the next subsection.

When $N_f = 2$, the $U(2)$ gauge field will generically be completely Higgsed. The gauge sector is trivial, and the precise nature of the resulting confined state is determined by whether the condensate of Φ spontaneously breaks any symmetry. Before the condensation, the system has a flavor rotation symmetry between Φ_1 and Φ_2 , which can maximally be $SU(2)$. The condensation pattern of $\Phi_{1,2}$ is dependent on the form of the quartic potential $V(\Phi)$ in Eq. (17). Specifically, if $V(\Phi)$ is $SU(2)$ invariant, it should have the form $\rho\text{Tr}M^2 + \lambda(\text{Tr}M)^2$, with $M_{IJ} = \sum_a \phi_{Ia}\phi_{Ja}^\dagger$. Here I, J are the flavor indices, and a is the color index. If $\rho, \lambda > 0$, Φ will condense in the $SU(2)$ invariant channel. In practice, the $SU(2)$ flavor symmetry is absent, but it is still possible that the condensation pattern of Φ does not break any physical symmetry, depending on the microscopic details. So we can end up with a completely trivial state with no topological order or spontaneous symmetry breaking.

Therefore, we have reached two continuum field theories for the confinement transitions of the ITO, with $N_f = 1, 2$, respectively. In both theories, in order to determine the symmetries of the confining states, we need to understand how the physical symmetries are embedded into the emergent symmetries of Eq. (15). Also, we need to know whether the physical symmetries are sufficient to forbid all other possibly relevant

operators with respect to these critical theories. In order to do this, a concrete microscopic construction of the critical theory is needed. It turns out to be easier to achieve this goal with a dual fermionic description to Eq. (15), as we will discuss below.

Before leaving this subsection, we point out an interesting relation between the theory Eq. (15) and the bosonic integer quantum Hall states (BIQH) [83, 84], although this relation is not of vital relevance for the discussions in this paper. The BIQH states are often viewed as bosonic SPTs protected by a $U(1)$ symmetry, but they are in fact compatible with a $U(2)$ symmetry. These states can be labelled by their Hall conductance under the $U(1)$ gauge field corresponding to the protecting $U(1)$ symmetry, $\sigma_{xy} = 2n$ with n an integer (in units such that the state described in Ref. [83] has $n = 1$). The response of the state with $n = -2$ to the $U(2)$ gauge field corresponding to the $U(2)$ symmetry is precisely given by (14) [83, 84]. In other words, the ITO can be obtained by gauging two copies of the BIQH states in Ref. [83], which is indeed similar to that the Abelian chiral spin liquid is a gauged (one-copy) BIQH state [85, 86]. Therefore, the theory Eq.(15) can be understood as condensing the bosons in the gauged BIQH states.

B. Symmetry properties and dual fermionic theories

The bosonic critical theory turns out to be dual to a fermionic critical theory,

$$\mathcal{L} = \sum_{I=1}^{N_f} \bar{\Psi}_I i(\not{\partial} - i\not{\mathbf{a}}) \Psi_I + m \sum \bar{\Psi}_I \Psi_I + \mathcal{L}_{\text{top}}, \quad (18)$$

$$\begin{aligned} \mathcal{L}_{\text{top}} = & \frac{2 - N_f/2}{4\pi} \text{Tr} \left[\mathbf{a} d\mathbf{a} - \frac{2i}{3} \mathbf{a}^3 \right] + (4 - N_f) \text{CS}_g \\ & + \frac{2}{4\pi} \beta d\beta - \frac{1}{2\pi} \beta d(B - (\text{Tra})). \end{aligned} \quad (19)$$

Here \mathbf{a} is a $U(2)$ gauge field, CS_g denotes the gravitational Chern-Simons term, β is a dynamical $U(1)$ gauge field, and B is a probe gauge field of the global $U(1)$ symmetry as in the bosonic critical theory. In our convention, when the coefficient of CS_g is 1, the theory has thermal Hall conductance $\kappa_{xy} = 1$ in units of $(\pi/6)(k_B^2 T/\hbar)$, or, in other words, it has an edge with chiral central charge $c_- = 1$. The fermion field Ψ is in the fundamental representation of the $U(2)$ gauge group, and its flavor number can be $N_f = 1, 2$. This duality can be derived using the level-rank duality [54] (see Appendix C), and it was also presented in Ref. [87]⁸.

Here the singlet mass of Dirac fermions $m \sum \bar{\Psi}_I \Psi_I$ is the tuning parameter of the confinement transition. When $m \ll -1$ (in proper units), integrating out the Dirac fermions gives a non-Abelian Chern-Simons theory,

$$\mathcal{L} = \frac{2}{4\pi} \text{Tr} \left[\mathbf{a} d\mathbf{a} - \frac{2i}{3} \mathbf{a}^3 \right] + 4\text{CS}_g + \frac{2}{4\pi} \beta d\beta + \frac{1}{2\pi} \beta d(\text{Tra}). \quad (20)$$

This theory indeed describes the ITO. One might be confused about this statement, since the Chern-Simons levels here look rather distinct from those in Eq. (15). However, it is inappropriate to directly compare the Chern-Simons levels between these two theories, because here \mathbf{a} is coupled to fermions, while \mathbf{b} in Eq. (15) is coupled to bosons. After taking into account the difference in the matter fields, we can show that the topological order of Eq. (20) is exactly the same as $U(2)_{2,-2}$ Chern-Simons theory, *i.e.*, the Ising TQFT. We can also do a quick self-consistent check by examining the gravitational response, whose coefficient corresponds to the physical thermal Hall conductance. The non-Abelian Chern-Simons term in Eq. (20) can be roughly considered as $U(2)_{-2} \times U(1)_{-2}$, and integrating out them yields a gravitational Chern-Simons term $-\frac{7}{2}\text{CS}_g$ ($U(2)_{-2}$ contributes $-\frac{5}{2}\text{CS}_g$ and $U(1)_{-2}$ contributes $-\text{CS}_g$). Combined with the 4CS_g term in (20), the total gravitational response is $\frac{1}{2}\text{CS}_g$, which is the identical to that of the ITO.

On the other hand, when $m \gg 1$, the ITO will be destroyed. As in the bosonic theories, the phases that ITO is confined to depend on the fermion flavor number N_f and the actions of the physical symmetries in these critical theories. More precisely, when $N_f = 1$, the theory will be confined to a pure $U(1)$ Maxwell theory, in which the monopole will proliferate and the nature of the resulting phase depends on the quantum numbers of the monopole. When $N_f = 2$, all the gauge fields will be confined without breaking any symmetry. This gives a trivially polarized state as long as there is no other relevant perturbation that can destroy the critical point. To understand the final fates of the confined states, we need to have concrete microscopic construction of the critical theories.

The above fermionic critical theories motivate a parton construction for the ITO and its confinement transitions. With such an explicit construction, we are able to directly work out the symmetry properties of the field theories. In particular, using our parton constructions, we will show that,

- i) The confined phase in the theory with $N_f = 1$ can indeed be the zigzag magnetic order.
- ii) The confined phase in the theory with $N_f = 2$ can indeed be a trivial state with all symmetries preserved.
- iii) The symmetries of the representative Kitaev materials (listed in Table I) are sufficient to for-

⁸ The duality only holds for $N_f = 1, 2$ [54].

bid the most obvious relevant operators in both critical theories (with $N_f = 1$ and $N_f = 2$, respectively).

To make the symmetries of Kitaev materials manifest, we consider a rotated spin basis,

$$\tilde{S}^x = \frac{S^x + S^y + S^z}{\sqrt{3}}, \quad (21)$$

$$\tilde{S}^y = \frac{S^x + S^y - 2S^z}{\sqrt{6}}, \quad (22)$$

$$\tilde{S}^z = \frac{S^x - S^y}{\sqrt{2}}. \quad (23)$$

Here $\tilde{S}^{x,y,z}$ are parallel to the c^* , a and b axis. The parton construction is [88]:

$$\tilde{S}^+ = \phi^\dagger f_a^\dagger f_b^\dagger, \quad \tilde{S}^z = \frac{n_\phi + n_{f_a} + n_{f_b}}{3} - \frac{1}{2}, \quad (24)$$

with a constraint $n_\phi = n_{f_a} = n_{f_b}$. This parton construction has a $U(2)$ gauge invariance: $\Psi = (f_a, f_b)^T$ is in the $U(2)$ fundamental representation, and it is interacting with a $U(2)$ gauge field \mathbf{a} ; ϕ carries charge under the diagonal part of the $U(2)$ gauge field and a global $U(1)$ charge (of the \tilde{S}_z rotation).

To get the ITO, we can put the bosonic parton ϕ into a Laughlin state at $\nu = -1/2$, and put the fermionic partons f_i into a topological band with Chern number $C = 2$. This gives exactly the Chern-Simons theory in Eq. (20): the fermionic parton contributes a $U(2)_{-2}$ Chern-Simons term for \mathbf{a} , while the bosonic parton is described by a $U(1)_{-2}$ Chern-Simons term of the $U(1)$ gauge field β .

The confinement transition of ITO can be triggered by changing the Chern number of fermionic partons. Specifically, for a transition from $C = 2$ to $C = 1$, we get a critical theory with $N_f = 1$, while for a transition from $C = 2$ to $C = 0$, we get a critical theory with $N_f = 2$. In Appendix D, we provide the concrete mean-field ansatz for these two Chern-number-changing transitions. We only consider a Zeeman field on the ac^* plane, which is the direction of Zeeman field reported in Ref. [26]. In this case, the symmetries of the system include translation $T_{1,2}$, inversion C_2 , as well as the combination of time-reversal and pseudo-mirror $\mathcal{T}\sigma^*$ (see Table I). We also work out how those symmetries are implemented in the critical theories using the mean-field ansatz.

In the theory with $N_f = 1$, besides the singlet mass (tuning parameter of the transition), the most relevant operators are the monopole operator \mathcal{M} , conserved current, $d(\text{Tra})$ and $\bar{\Psi}\gamma^\mu\Psi$. Their quantum numbers are shown in Table III, and all of them are disallowed by symmetries. The minimally allowed monopole operator is a two-fold monopole, which may or may not be relevant in the infrared. If it is irrelevant, we may have a stable critical point with an emergent $U(2)$ gauge field. Furthermore, the monopole has exactly the same

	T_1	T_2	C_2	$\mathcal{T}\sigma^*$
\mathcal{M}	-1	-1	-1	$-\mathcal{M}^\dagger$
$\bar{\Psi}\gamma^0\Psi$	1	1	1	-1
$\bar{\Psi}\gamma^1\Psi$	1	1	-1	1
$\bar{\Psi}\gamma^2\Psi$	1	1	-1	-1

TABLE III. Symmetries of operators in the $N_f = 1$ critical theory. $d(\text{Tra})$ happens to have the same quantum number as $\bar{\Psi}\gamma^\mu\Psi$.

quantum number as the zigzag magnetic order, assuming the magnetic moments are ordered on the ac^* plane in the zigzag phase, as suggested by Refs. [15, 58]. Therefore, the proliferation of monopoles in the theory with $N_f = 1$ results in precisely the zigzag magnetic order.

We now turn to the critical theory with $N_f = 2$. Besides the $U(1)$ flux conservation, the critical theory also has an $SU(2)$ flavor rotation symmetry. The most relevant operators are the monopole operator $\mathcal{M}_{1,2,3}$, $SU(2)$ adjoint mass $\bar{\Psi}\tau^\alpha\Psi$ (τ acts on the flavor index), and conserved currents, $d(\text{Tra})$, $\bar{\Psi}\gamma^\mu\tau^\alpha\Psi$ and $\bar{\Psi}\gamma^\mu\Psi$. Here the monopoles are in the adjoint representation of the $SU(2)$ flavor symmetry, and it has three components. Again, we want to work out the quantum numbers of these operators to see if they are forbidden by symmetries. There turn out to be three different cases, depending on the locations of Dirac cones. Constrained by symmetries, the two Dirac points have to stay at the high symmetry points/lines (see Fig. 7):

1. The two Dirac cones are at the $M_{1,2}$ points, $(k_1, k_2) = (\pi, 0), (0, \pi)$.
2. The two Dirac cones are at $(k_1, k_2) = (k, k), (-k, -k)$ points (k is an arbitrary number), which are on the high symmetry line $K-K'$.
3. The two Dirac cones are at $(k_1, k_2) = (k, -k), (-k, k)$ points (k is an arbitrary number), which are on the high symmetric line $M_3 - M_3$.

In Appendix D, we provide the mean-field ansatz for all the three possibilities, and the quantum numbers of operators are summarized in Table IV-VI.

In case (1) (the nodes are located at $M_{1,2}$ points), there is one symmetry allowed operator, $\bar{\Psi}\gamma^0\tau^z\Psi = \Psi_1^\dagger\Psi_1 - \Psi_2^\dagger\Psi_2$. This operator will destabilize the quantum critical point: it will dope the Dirac cones at the M_1, M_2 points and generate particle and hole pockets. These two Fermi pockets are interacting with a $U(2)$ gauge field, which may or may not be stable. In cases (2) and (3), again there is one symmetry allowed relevant operator: $\bar{\Psi}\gamma^1\tau^z\Psi$ and $\bar{\Psi}\gamma^2\tau^z\Psi$, respectively. However, different from the first situation, these operators will not destroy the quantum critical points.

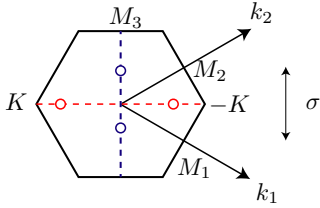


FIG. 7. Brillouin zone of the honeycomb lattice. The red dashed line represents the high symmetric line which connects the K and $K' = -K$ point; The blue dashed line connects the M_3 and M_3 point.

Instead, they will just move the Dirac points along the high symmetry lines (along either the K - K' or the M_3 - M_3 line). Therefore, the quantum critical point between the ITO and polarized state may be stable if the two Dirac nodes are staying at the high symmetric lines.

V. Discussion

Motivated by the recent theoretical and experimental progress in the research on Kitaev materials, we have studied the phase diagram of Kitaev materials. Within the Kitaev model subject to a Zeeman field, we have numerically demonstrated that, in addition to the trivial polarized state and the Ising topologically ordered (ITO) state, another exotic quantum spin liquid state with neutral Fermi surfaces (NFS) appears in certain range of the field strengths. This state can be described by Fermi pockets of emergent electrically neutral spinons coupled to an emergent dynamical $U(1)$ gauge field. We have presented a parton construction of this NFS state, and described the quantum phase transitions from this state to the trivial polarized state and to the ITO state. These phase transitions can be understood in terms of Lifshitz transition and pairing transition of the spinons coupled to the emergent $U(1)$ gauge field, respectively.

The real Kitaev materials have very complex structures for the spin-spin interactions [89, 90], and it will be certainly very helpful to understand the ground states in more realistic models. Although our numerical model is based on an idealized antiferromagnetic Kitaev model under a Zeeman field, we expect the qualitative features of our results to hold for various real Kitaev materials, especially the ones that can realize ITO under a finite Zeeman field. Therefore, it is important to experimentally determine whether the real materials realize the exotic phases discussed here.

One of the experimental signatures of the NFS state is that the specific heat and longitudinal thermal conductance (with phonon contributions subtracted) at the lowest temperatures should increase significantly when the system enters this phase from the ITO state. Within this phase, these quantities should qualitatively

have power-law temperature dependence with some anomalous exponents. Because of the existence of a neutral Fermi surface, the spin-spin correlation functions will show signatures of $2k_f$ singularities. Therefore, neutron scattering can be used to detect this NFS state, as is done in the material YbMgGaO_4 [46]. This can be a method to distinguish the NFS state and the Z_2 gapless Majorana cone state in the pure Kitaev model [68, 91, 92]. Perhaps more striking phenomena of this state are the possible quantum magnetic oscillations and charge Friedel oscillations in this electric insulator [93–95]. These oscillating behaviors were first discussed in the context of the organic compound κ -(BEDT-TTF) $_2\text{Cu}_2(\text{CN})_3$, which is known to be a weak Mott insulator, in the sense that it is close to a metal-insulator transition [96]. On the other hand, Kitaev materials such as α - RuCl_3 are strong Mott insulators [97, 98], so we expect quantitative differences on these oscillating effects therein from the organic compound.

We have further studied the transitions from the ITO state to the zigzag order and to the trivial polarized state. We find that these transitions can be described by QCD $_3$ -Chern-Simons theories. In particular, the transition between the ITO and the zigzag order (the trivial polarized state) can be described by a dynamical $U(2)$ gauge field coupled to $N_f = 1$ ($N_f = 2$) critical fermions. We have checked that the symmetries of some representative Kitaev materials (listed in Table I) are sufficient to forbid the most obvious relevant operators of these putative critical theories. Therefore, these transitions can potentially be generic direct continuous quantum phase transitions. We note that our method can also be adopted to study the transitions between the ITO and magnetic orders other than the zigzag type.

We also note that these critical theories are dual to $N_f = 1$ ($N_f = 2$) species of critical bosons coupled to a dynamical $U(2)$ gauge field. There is an interesting relation between these critical theories with bosonic integer quantum Hall (BIQH) states. The quantum phase transitions from the BIQH states to a superfluid and to a trivial insulator have been widely studied in recent years [99–101], and it may be worth relating these transitions to the transitions from the ITO state to other states.

The critical theories presented in this paper are all beyond the conventional paradigm of phase transitions, and it is worth studying them in more depth. On the experimental front, it is helpful to examine the phase diagrams of the Kitaev materials more closely, and identify different phases and study the phase transitions. Numerically, it is important to study the phase diagram of more realistic lattice models. In the purely theoretical direction, it will be of interest to study the low-energy dynamics of these critical theories to determine whether these transitions can be continuous, and what the critical exponents are. These studies will provide further insights to the experimental studies of the

Kitaev materials. Also, given the similarities among the critical theories between different pairs of phases, it may be interesting to look for a theory of a multi-critical point that becomes these phases and critical theories upon adding perturbations. This will potentially lead to unified understanding of the rich structures of the quantum magnetism in these systems.

Finally, we remark that dualities and emergent non-Abelian gauge theories similar to ours may be useful tools to understand other types of exotic quantum phases and phase transitions in condensed matter systems, and we expect more applications of related ideas will arrive in the future and be proved helpful.

VI. Acknowledgement

We thank for inspiring discussions with Lukas Janssen, Itamar Kimchi, Sung-Sik Lee, Max Metlitski, T. Senthil, Ashvin Vishwananth, and Chong Wang. We thank Yuan-Ming Lu for sharing unpublished paper. L. Z. was supported by NSF grant DMR-1608505. L. Z. thanks Perimeter Institute for Theoretical Physics for hospitality, where part of this work was done. This research was supported in part by Perimeter Institute for Theoretical Physics. Research at Perimeter Institute is supported by the Government of Canada through the Department of Innovation, Science and Economic Development Canada and by the Province of Ontario through the Ministry of Research, Innovation and Science.

Note added: Upon the completion of this project, we became aware of an independent work by H.-C. Jiang, C.-Y. Wang, B. Huang, and Y.-M. Lu, which studies the field induced NFS state in the Kitaev model [102].

-
- [1] Xiao-Gang Wen, *Quantum field theory of many-body systems* (Oxford University Press, 2004).
 - [2] Subir Sachdev, *Quantum Phase Transitions*, 2nd ed. (Cambridge University Press, 2011).
 - [3] Alexei Kitaev, “Anyons in an exactly solved model and beyond,” *Annals of Physics* **321**, 2 – 111 (2006), january Special Issue.
 - [4] Chetan Nayak, Steven H. Simon, Ady Stern, Michael Freedman, and Sankar Das Sarma, “Non-abelian anyons and topological quantum computation,” *Rev. Mod. Phys.* **80**, 1083–1159 (2008).
 - [5] Giniyat Khaliullin, “Orbital order and fluctuations in mott insulators,” *Progress of Theoretical Physics Supplement* **160**, 155–202 (2005).
 - [6] G. Jackeli and G. Khaliullin, “Mott insulators in the strong spin-orbit coupling limit: From heisenberg to a quantum compass and kitaev models,” *Phys. Rev. Lett.* **102**, 017205 (2009).
 - [7] Jiří Chaloupka, George Jackeli, and Giniyat Khaliullin, “Kitaev-heisenberg model on a honeycomb lattice: Possible exotic phases in iridium oxides $A_2\text{IrO}_3$,” *Phys. Rev. Lett.* **105**, 027204 (2010).
 - [8] Jeffrey G. Rau, Eric Kin-Ho Lee, and Hae-Young Kee, “Spin-orbit physics giving rise to novel phases in correlated systems: Iridates and related materials,” *Annual Review of Condensed Matter Physics* **7**, 195–221 (2016), <https://doi.org/10.1146/annurev-conmatphys-031115-011319>.
 - [9] S. Trebst, “Kitaev Materials,” ArXiv e-prints (2017), [arXiv:1701.07056 \[cond-mat.str-el\]](https://arxiv.org/abs/1701.07056).
 - [10] S. M. Winter, A. A. Tsirlin, M. Daghofer, J. van den Brink, Y. Singh, P. Gegenwart, and R. Valentí, “Models and materials for generalized Kitaev magnetism,” *Journal of Physics Condensed Matter* **29**, 493002 (2017), [arXiv:1706.06113 \[cond-mat.str-el\]](https://arxiv.org/abs/1706.06113).
 - [11] J. M. Fletcher, W. E. Gardner, A. C. Fox, and G. Topping, “X-ray, infrared, and magnetic studies of - and -ruthenium trichloride,” *J. Chem. Soc. A*, 1038–1045 (1967).
 - [12] Y. Kobayashi, T. Okada, K. Asai, M. Katada, H. Sano, and F. Ambe, “Moessbauer spectroscopy and magnetization studies of .alpha.- and .beta.-ruthenium trichloride,” *Inorganic Chemistry* **31**, 4570–4574 (1992), <https://doi.org/10.1021/ic00048a025>.
 - [13] J. A. Sears, M. Songvilay, K. W. Plumb, J. P. Clancy, Y. Qiu, Y. Zhao, D. Parshall, and Young-June Kim, “Magnetic order in $\alpha - \text{ruCl}_3$: A honeycomb-lattice quantum magnet with strong spin-orbit coupling,” *Phys. Rev. B* **91**, 144420 (2015).
 - [14] R. D. Johnson, S. C. Williams, A. A. Haghighirad, J. Singleton, V. Zapf, P. Manuel, I. I. Mazin, Y. Li, H. O. Jeschke, R. Valentí, and R. Coldea, “Monoclinic crystal structure of $\alpha - \text{ruCl}_3$ and the zigzag antiferromagnetic ground state,” *Phys. Rev. B* **92**, 235119 (2015).
 - [15] H. B. Cao, A. Banerjee, J.-Q. Yan, C. A. Bridges, M. D. Lumsden, D. G. Mandrus, D. A. Tennant, B. C. Chakoumakos, and S. E. Nagler, “Low-temperature crystal and magnetic structure of $\alpha - \text{ruCl}_3$,” *Phys. Rev. B* **93**, 134423 (2016).
 - [16] J. Chaloupka, G. Jackeli, and G. Khaliullin, “Zigzag Magnetic Order in the Iridium Oxide Na_2IrO_3 ,” *Physical Review Letters* **110**, 097204 (2013), [arXiv:1209.5100 \[cond-mat.str-el\]](https://arxiv.org/abs/1209.5100).
 - [17] Jeffrey G. Rau, Eric Kin-Ho Lee, and Hae-Young Kee, “Generic spin model for the honeycomb iridates beyond the kitaev limit,” *Phys. Rev. Lett.* **112**, 077204 (2014).
 - [18] M. Gohlke, G. Wachtel, Y. Yamaji, F. Pollmann, and Y. B. Kim, “Quantum spin liquid signatures in Kitaev-like frustrated magnets,” *Phys. Rev. B* **97**, 075126 (2018), [arXiv:1706.09908 \[cond-mat.str-el\]](https://arxiv.org/abs/1706.09908).
 - [19] X. Liu, T. Berlijn, W.-G. Yin, W. Ku, A. Tsve-

- lik, Young-June Kim, H. Gretarsson, Yogesh Singh, P. Gegenwart, and J. P. Hill, “Long-range magnetic ordering in Na_2IrO_3 ,” *Phys. Rev. B* **83**, 220403 (2011).
- [20] S. K. Choi, R. Coldea, A. N. Kolmogorov, T. Lancaster, I. I. Mazin, S. J. Blundell, P. G. Radaelli, Yogesh Singh, P. Gegenwart, K. R. Choi, S.-W. Cheong, P. J. Baker, C. Stock, and J. Taylor, “Spin waves and revised crystal structure of honeycomb iridate Na_2IrO_3 ,” *Phys. Rev. Lett.* **108**, 127204 (2012).
- [21] Feng Ye, Songxue Chi, Huibo Cao, Bryan C. Chakoumakos, Jaime A. Fernandez-Baca, Radu Custelcean, T. F. Qi, O. B. Korneta, and G. Cao, “Direct evidence of a zigzag spin-chain structure in the honeycomb lattice: A neutron and x-ray diffraction investigation of single-crystal Na_2IrO_3 ,” *Phys. Rev. B* **85**, 180403 (2012).
- [22] Arnab Banerjee, Jiaqiang Yan, Johannes Knolle, Craig A Bridges, Matthew B Stone, Mark D Lumsden, David G Mandrus, David A Tennant, Roderich Moessner, and Stephen E Nagler, “Neutron scattering in the proximate quantum spin liquid $\alpha\text{-RuCl}_3$,” *Science* **356**, 1055–1059 (2017).
- [23] P. Lampen-Kelley, L. Janssen, E. C. Andrade, S. Rachel, J.-Q. Yan, C. Balz, D. G. Mandrus, S. E. Nagler, and M. Vojta, “Field-induced intermediate phase in $\alpha\text{-RuCl}_3$: Non-coplanar order, phase diagram, and proximate spin liquid,” ArXiv e-prints (2018), [arXiv:1807.06192 \[cond-mat.str-el\]](#).
- [24] Nejc Janša, Andrej Zorko, Matjaž Gomilšek, Matej Pregelj, Karl W. Krämer, Daniel Biner, Alun Biffin, Christian Rüegg, and Martin Klanjšek, “Observation of two types of fractional excitation in the kitaev honeycomb magnet,” *Nature Physics* **14**, 786–790 (2018).
- [25] Arnab Banerjee, Paula Lampen-Kelley, Johannes Knolle, Christian Balz, Adam Anthony Aczel, Barry Winn, Yaohua Liu, Daniel Pajerowski, Jiaqiang Yan, Craig A. Bridges, Andrei T. Savici, Bryan C. Chakoumakos, Mark D. Lumsden, David Alan Tennant, Roderich Moessner, David G. Mandrus, and Stephen E. Nagler, “Excitations in the field-induced quantum spin liquid state of $\alpha\text{-RuCl}_3$,” *npj Quantum Materials* **3**, 8 (2018).
- [26] Y. Kasahara, T. Ohnishi, Y. Mizukami, O. Tanaka, S. Ma, K. Sugii, N. Kurita, H. Tanaka, J. Nasu, Y. Motome, T. Shibauchi, and Y. Matsuda, “Majorana quantization and half-integer thermal quantum Hall effect in a Kitaev spin liquid,” ArXiv e-prints (2018), [arXiv:1805.05022 \[cond-mat.str-el\]](#).
- [27] M. Ye, G. B. Halász, L. Savary, and L. Balents, “Quantization of the thermal Hall conductivity at small Hall angles,” ArXiv e-prints (2018), [arXiv:1805.10532 \[cond-mat.str-el\]](#).
- [28] Yuval Vinkler-Aviv and Achim Rosch, “Approximately quantized thermal hall effect of chiral liquids coupled to phonons,” *Phys. Rev. X* **8**, 031032 (2018).
- [29] J. Cookmeyer and J. E. Moore, “Spin Wave Analysis of Low-Temperature Thermal Hall Effect in the Candidate Kitaev Spin Liquid $\alpha\text{-RuCl}_3$,” ArXiv e-prints (2018), [arXiv:1807.03857 \[cond-mat.str-el\]](#).
- [30] C. Hickey and S. Trebst, “Gapless Visions and Emergent U(1) Spin Liquid in the Kitaev Honeycomb Model: Complete Phase Diagram in Tilted Magnetic Fields,” ArXiv e-prints (2018), [arXiv:1805.05953 \[cond-mat.str-el\]](#).
- [31] M. Gohlke, R. Moessner, and F. Pollmann, “Dynamical and topological properties of the Kitaev model in a [111] magnetic field,” *Phys. Rev. B* **98**, 014418 (2018), [arXiv:1804.06811 \[cond-mat.str-el\]](#).
- [32] Zheng Zhu, Itamar Kimchi, D. N. Sheng, and Liang Fu, “Robust non-abelian spin liquid and a possible intermediate phase in the antiferromagnetic kitaev model with magnetic field,” *Phys. Rev. B* **97**, 241110 (2018).
- [33] Patrick A. Lee, Naoto Nagaosa, and Xiao-Gang Wen, “Doping a mott insulator: Physics of high-temperature superconductivity,” *Rev. Mod. Phys.* **78**, 17–85 (2006).
- [34] G. Baskaran, Z. Zou, and P.W. Anderson, “The resonating valence bond state and high- T_c superconductivity a mean field theory,” *Solid State Communications* **63**, 973 – 976 (1987).
- [35] Ian Affleck and J. Brad Marston, “Large- n limit of the heisenberg-hubbard model: Implications for high- T_c superconductors,” *Phys. Rev. B* **37**, 3774–3777 (1988).
- [36] Patrick A. Lee and Naoto Nagaosa, “Gauge theory of the normal state of high- T_c superconductors,” *Phys. Rev. B* **46**, 5621–5639 (1992).
- [37] Xiao-Gang Wen and Patrick A. Lee, “Theory of underdoped cuprates,” *Phys. Rev. Lett.* **76**, 503–506 (1996).
- [38] Sung-Sik Lee and Patrick A. Lee, “U(1) gauge theory of the hubbard model: Spin liquid states and possible application to $\kappa\text{-(BEDT-TTF)}_2\text{Cu}_2(\text{CN})_3$,” *Phys. Rev. Lett.* **95**, 036403 (2005).
- [39] Sung-Sik Lee, “Stability of the u(1) spin liquid with a spinon fermi surface in 2 + 1 dimensions,” *Phys. Rev. B* **78**, 085129 (2008).
- [40] Sung-Sik Lee, “Low-energy effective theory of fermi surface coupled with u(1) gauge field in 2 + 1 dimensions,” *Phys. Rev. B* **80**, 165102 (2009).
- [41] T. Senthil, “Theory of a continuous mott transition in two dimensions,” *Phys. Rev. B* **78**, 045109 (2008).
- [42] David F. Mross, John McGreevy, Hong Liu, and T. Senthil, “Controlled expansion for certain non-fermi-liquid metals,” *Phys. Rev. B* **82**, 045121 (2010).
- [43] Max A. Metlitski, David F. Mross, Subir Sachdev, and T. Senthil, “Cooper pairing in non-fermi liquids,” *Phys. Rev. B* **91**, 115111 (2015).
- [44] Liujun Zou and T. Senthil, “Dimensional decoupling at continuous quantum critical mott transitions,” *Phys. Rev. B* **94**, 115113 (2016).
- [45] Y. Shimizu, K. Miyagawa, K. Kanoda, M. Maesato, and G. Saito, “Spin liquid state in an organic mott insulator with a triangular lattice,” *Phys. Rev. Lett.* **91**, 107001 (2003).
- [46] Yao Shen, Yao-Dong Li, Hongliang Wo, Yuesheng Li, Shoudong Shen, Bingying Pan, Qisi Wang, H. C. Walker, P. Steffens, M. Boehm, Yiqing Hao, D. L. Quintero-Castro, L. W. Harriger, M. D. Frontzek, Lijie Hao, Siqin Meng, Qingming Zhang, Gang Chen, and Jun Zhao, “Evidence for a spinon fermi surface in a triangular-lattice quantum-spin-liquid candidate,” *Nature* **540**, 559 EP – (2016).
- [47] Itamar Kimchi, Adam Nahum, and T. Senthil, “Valence bonds in random quantum magnets: Theory and application to YbMgGaO_4 ,” *Phys. Rev. X* **8**, 031028 (2018).

- [48] A. U. B. Wolter, L. T. Corredor, L. Janssen, K. Nenkov, S. Schönecker, S.-H. Do, K.-Y. Choi, R. Albrecht, J. Hunger, T. Doert, M. Vojta, and B. Büchner, “Field-induced quantum criticality in the Kitaev system α -RuCl₃,” *Phys. Rev. B* **96**, 041405 (2017), [arXiv:1704.03475 \[cond-mat.str-el\]](#).
- [49] Dam Thanh Son, “Is the composite fermion a dirac particle?” *Phys. Rev. X* **5**, 031027 (2015).
- [50] Chong Wang and T. Senthil, “Dual dirac liquid on the surface of the electron topological insulator,” *Phys. Rev. X* **5**, 041031 (2015).
- [51] M. A. Metlitski and A. Vishwanath, “Particle-vortex duality of two-dimensional Dirac fermion from electric-magnetic duality of three-dimensional topological insulators,” *Phys. Rev. B* **93**, 245151 (2016).
- [52] Nathan Seiberg, T. Senthil, Chong Wang, and Edward Witten, “A duality web in dimensions and condensed matter physics,” *Annals of Physics* **374**, 395 – 433 (2016).
- [53] A. Karch and D. Tong, “Particle-Vortex Duality from 3D Bosonization,” *Physical Review X* **6**, 031043 (2016), [arXiv:1606.01893 \[hep-th\]](#).
- [54] Po-Shen Hsin and Nathan Seiberg, “Level/rank duality and chern-simons-matter theories,” *Journal of High Energy Physics* **2016**, 95 (2016).
- [55] J. Y. Lee, C. Wang, M. P. Zaletel, A. Vishwanath, and Y.-C. He, “Emergent Multi-Flavor QED₃ at the Plateau Transition between Fractional Chern Insulators: Applications to Graphene Heterostructures,” *Physical Review X* **8**, 031015 (2018), [arXiv:1802.09538 \[cond-mat.str-el\]](#).
- [56] S.-Y. Park, S.-H. Do, K.-Y. Choi, D. Jang, T.-H. Jang, J. Schefer, C.-M. Wu, J. S. Gardner, J. M. S. Park, J.-H. Park, and S. Ji, “Emergence of the Isotropic Kitaev Honeycomb Lattice with Two-dimensional Ising Universality in $\{\alpha\}$ -RuCl₃,” *ArXiv e-prints* (2016), [arXiv:1609.05690 \[cond-mat.mtrl-sci\]](#).
- [57] Seung-Hwan Do, Sang-Youn Park, Junki Yoshitake, Joji Nasu, Yukitoshi Motome, Yong Seung Kwon, D. T. Adroja, D. J. Voneshen, Kyoo Kim, T. H. Jang, J. H. Park, Kwang-Yong Choi, and Sungdae Ji, “Majorana fermions in the kitaev quantum spin system -rucl₃,” *Nature Physics* **13**, 1079 EP – (2017).
- [58] S. H. Chun, J.-W. Kim, J. Kim, H. Zheng, C. C. Stoumpos, C. D. Malliakas, J. F. Mitchell, K. Mehlawat, Y. Singh, Y. Choi, T. Gog, A. Al-Zein, M. Moretti Sala, M. Krisch, J. Chaloupka, G. Jackeli, G. Khaliullin, and B. J. Kim, “Direct Evidence for Dominant Bond-directional Interactions in a Honeycomb Lattice Iridate Na₂IrO₃,” *ArXiv e-prints* (2015), [arXiv:1504.03618 \[cond-mat.mtrl-sci\]](#).
- [59] Steven R. White, “Density matrix formulation for quantum renormalization groups,” *Phys. Rev. Lett.* **69**, 2863–2866 (1992).
- [60] Steven R. White, “Density-matrix algorithms for quantum renormalization groups,” *Phys. Rev. B* **48**, 10345–10356 (1993).
- [61] I. P. McCulloch, “Infinite size density matrix renormalization group, revisited,” *ArXiv e-prints* (2008), [arXiv:0804.2509 \[cond-mat.str-el\]](#).
- [62] H.-C. Jiang, Z.-C. Gu, X.-L. Qi, and S. Trebst, “Possible proximity of the Mott insulating iridate Na₂IrO₃ to a topological phase: Phase diagram of the Heisenberg-Kitaev model in a magnetic field,” *Phys. Rev. B* **83**, 245104 (2011), [arXiv:1101.1145 \[cond-mat.str-el\]](#).
- [63] D. N. Sheng, Olexei I. Motrunich, and Matthew P. A. Fisher, “Spin bose-metal phase in a spin- $\frac{1}{2}$ model with ring exchange on a two-leg triangular strip,” *Phys. Rev. B* **79**, 205112 (2009).
- [64] Frank Pollmann, Subroto Mukerjee, Ari M. Turner, and Joel E. Moore, “Theory of finite-entanglement scaling at one-dimensional quantum critical points,” *Phys. Rev. Lett.* **102**, 255701 (2009).
- [65] S. D. Geraedts, C. Repellin, C. Wang, R. S. K. Mong, T. Senthil, and N. Regnault, “Emergent particle-hole symmetry in spinful bosonic quantum Hall systems,” *Phys. Rev. B* **96**, 075148 (2017), [arXiv:1704.01594 \[cond-mat.str-el\]](#).
- [66] Yin-Chen He, Michael P. Zaletel, Masaki Oshikawa, and Frank Pollmann, “Signatures of dirac cones in a dmrg study of the kagome heisenberg model,” *Phys. Rev. X* **7**, 031020 (2017).
- [67] V. Zauner, D. Draxler, L. Vanderstraeten, M. Degroote, J. Haegeman, M. M. Rams, V. Stojevic, N. Schuch, and F. Verstraete, “Transfer matrices and excitations with matrix product states,” *New Journal of Physics* **17**, 053002 (2015).
- [68] J. Knolle, D. L. Kovrizhin, J. T. Chalker, and R. Moessner, “Dynamics of a Two-Dimensional Quantum Spin Liquid: Signatures of Emergent Majorana Fermions and Fluxes,” *Physical Review Letters* **112**, 207203 (2014), [arXiv:1308.4336 \[cond-mat.str-el\]](#).
- [69] A.M. Polyakov, “Quark confinement and topology of gauge theories,” *Nuclear Physics B* **120**, 429 – 458 (1977).
- [70] Patrick A. Lee, Naoto Nagaosa, and Xiao-Gang Wen, “Doping a mott insulator: Physics of high-temperature superconductivity,” *Rev. Mod. Phys.* **78**, 17–85 (2006).
- [71] F. J. Burnell and Chetan Nayak, “Su(2) slave fermion solution of the kitaev honeycomb lattice model,” *Phys. Rev. B* **84**, 125125 (2011).
- [72] Yi-Zhuang You, Itamar Kimchi, and Ashvin Vishwanath, “Doping a spin-orbit mott insulator: Topological superconductivity from the kitaev-heisenberg model and possible application to (na₂/li₂)iro₃,” *Phys. Rev. B* **86**, 085145 (2012).
- [73] Victor Chua, Hong Yao, and Gregory A. Fiete, “Exact chiral spin liquid with stable spin fermi surface on the kagome lattice,” *Phys. Rev. B* **83**, 180412 (2011).
- [74] X.-Y. Song and et. al. (in prepare), .
- [75] Takahiro Fukui, Yasuhiro Hatsugai, and Hiroshi Suzuki, “Chern numbers in discretized brillouin zone: Efficient method of computing (spin) hall conductances,” *Journal of the Physical Society of Japan* **74**, 1674–1677 (2005), [https://doi.org/10.1143/JPSJ.74.1674](#).
- [76] Fiona Burnell, Xie Chen, Alexei Kitaev, Max Metlitski, and Ashvin Vishwanath, “Time reversal invariant gapped boundaries of the double semion state,” *Phys. Rev. B* **93**, 235161 (2016).
- [77] Chong Wang and T. Senthil, “Time-reversal symmetric $u(1)$ quantum spin liquids,” *Phys. Rev. X* **6**, 011034 (2016).
- [78] Liujun Zou, Chong Wang, and T. Senthil, “Symme-

- try enriched $u(1)$ quantum spin liquids,” *Phys. Rev. B* **97**, 195126 (2018).
- [79] Liujun Zou, “Bulk characterization of topological crystalline insulators: Stability under interactions and relations to symmetry enriched $u(1)$ quantum spin liquids,” *Phys. Rev. B* **97**, 045130 (2018).
- [80] N. Read and Subir Sachdev, “Large- n expansion for frustrated quantum antiferromagnets,” *Phys. Rev. Lett.* **66**, 1773–1776 (1991).
- [81] N. Seiberg and E. Witten, “Gapped boundary phases of topological insulators via weak coupling,” *Progress of Theoretical and Experimental Physics* **2016**, 12C101 (2016), arXiv:1602.04251 [cond-mat.str-el].
- [82] C. Dasgupta and B. I. Halperin, “Phase transition in a lattice model of superconductivity,” *Phys. Rev. Lett.* **47**, 1556–1560 (1981).
- [83] T. Senthil and Michael Levin, “Integer quantum hall effect for bosons,” *Phys. Rev. Lett.* **110**, 046801 (2013).
- [84] Zheng-Xin Liu and Xiao-Gang Wen, “Symmetry-protected quantum spin hall phases in two dimensions,” *Phys. Rev. Lett.* **110**, 067205 (2013).
- [85] M. Barkeshli, “Transitions Between Chiral Spin Liquids and Z₂ Spin Liquids,” ArXiv e-prints (2013), arXiv:1307.8194 [cond-mat.str-el].
- [86] Yin-Chen He, Subhro Bhattacharjee, Frank Pollmann, and R. Moessner, “Kagome chiral spin liquid as a gauged $u(1)$ symmetry protected topological phase,” *Phys. Rev. Lett.* **115**, 267209 (2015).
- [87] D. Radičević, D. Tong, and C. Turner, “Non-abelian 3 D bosonization and quantum Hall states,” *Journal of High Energy Physics* **12**, 67 (2016), arXiv:1608.04732 [hep-th].
- [88] X. G. Wen, “Non-abelian statistics in the fractional quantum hall states,” *Phys. Rev. Lett.* **66**, 802–805 (1991).
- [89] Lukas Janssen, Eric C. Andrade, and Matthias Vojta, “Honeycomb-lattice heisenberg-kitaev model in a magnetic field: Spin canting, metamagnetism, and vortex crystals,” *Phys. Rev. Lett.* **117**, 277202 (2016).
- [90] Lukas Janssen, Eric C. Andrade, and Matthias Vojta, “Magnetization processes of zigzag states on the honeycomb lattice: Identifying spin models for α -rucl₃ and na₂iro₃,” *Phys. Rev. B* **96**, 064430 (2017).
- [91] X.-Y. Song, Y.-Z. You, and L. Balents, “Low-Energy Spin Dynamics of the Honeycomb Spin Liquid Beyond the Kitaev Limit,” *Physical Review Letters* **117**, 037209 (2016), arXiv:1604.04365 [cond-mat.str-el].
- [92] M. Gohlke, R. Verresen, R. Moessner, and F. Pollmann, “Dynamics of the Kitaev-Heisenberg Model,” *Physical Review Letters* **119**, 157203 (2017), arXiv:1701.04678 [cond-mat.str-el].
- [93] Olexei I. Motrunich, “Orbital magnetic field effects in spin liquid with spinon fermi sea: Possible application to κ -(ET)₂cu₂(CN)₃,” *Phys. Rev. B* **73**, 155115 (2006).
- [94] David F. Mross and T. Senthil, “Charge friedel oscillations in a mott insulator,” *Phys. Rev. B* **84**, 041102 (2011).
- [95] Inti Sodemann, Debanjan Chowdhury, and T. Senthil, “Quantum oscillations in insulators with neutral fermi surfaces,” *Phys. Rev. B* **97**, 045152 (2018).
- [96] Y. Kurosaki, Y. Shimizu, K. Miyagawa, K. Kanoda, and G. Saito, “Mott transition from a spin liquid to a fermi liquid in the spin-frustrated organic conductor κ -(ET)₂cu₂(CN)₃,” *Phys. Rev. Lett.* **95**, 177001 (2005).
- [97] K. W. Plumb, J. P. Clancy, L. J. Sandilands, V. Vijay Shankar, Y. F. Hu, K. S. Burch, Hae-Young Kee, and Young-June Kim, “ α -rucl₃: A spin-orbit assisted mott insulator on a honeycomb lattice,” *Phys. Rev. B* **90**, 041112 (2014).
- [98] Xiaoqing Zhou, Haoxiang Li, J. A. Waugh, S. Parham, Heung-Sik Kim, J. A. Sears, A. Gomes, Hae-Young Kee, Young-June Kim, and D. S. Dessau, “Angle-resolved photoemission study of the kitaev candidate α -rucl₃,” *Phys. Rev. B* **94**, 161106 (2016).
- [99] Tarun Grover and Ashvin Vishwanath, “Quantum phase transition between integer quantum hall states of bosons,” *Phys. Rev. B* **87**, 045129 (2013).
- [100] Yuan-Ming Lu and Dung-Hai Lee, “Quantum phase transitions between bosonic symmetry-protected topological phases in two dimensions: Emergent qed₃ and anyon superfluid,” *Phys. Rev. B* **89**, 195143 (2014).
- [101] C. Wang, A. Nahum, M. A. Metlitski, C. Xu, and T. Senthil, “Deconfined quantum critical points: symmetries and dualities,” ArXiv e-prints (2017), arXiv:1703.02426 [cond-mat.str-el].
- [102] H.-C. Jiang, C.-Y. Wang, B. Huang, and Y.-M. Lu, “Field induced quantum spin liquid with spinon Fermi surfaces in the Kitaev model,” ArXiv e-prints (2018), arXiv:1809.08247 [cond-mat.str-el].
- [103] Vadim Borokhov, Anton Kapustin, and Xinkai Wu, “Topological disorder operators in three-dimensional conformal field theory,” *Journal of High Energy Physics* **2002**, 049 (2002).
- [104] J. Alicea, “Monopole quantum numbers in the staggered flux spin liquid,” *Phys. Rev. B* **78**, 035126 (2008), arXiv:0804.0786 [cond-mat.str-el].

A. Symmetry actions of the Kitaev model and the neutral Fermi surface state

In this appendix we review the symmetry actions of the Kitaev model, and present a gauge transformation that converts them into the symmetry actions in Table II.

The symmetry actions of the Kitaev model are discussed in details in Ref. [72]. For completeness, let us first review the relevant results therein. Ref. [72] also starts from the parton construction given by (6), but in a way where the $SU(2)$ gauge structure is manifest. More precisely, on the site i define

$$F_i = \begin{pmatrix} f_{i1} & -f_{i2}^\dagger \\ f_{i2} & f_{i1}^\dagger \end{pmatrix} \quad (\text{A1})$$

so that the physical spin operators on this site can be written in terms of F_i as

$$\mathbf{S}_i = \frac{1}{4} \text{Tr} \left(F_i^\dagger \boldsymbol{\sigma} F_i \right) \quad (\text{A2})$$

Because (A2) is invariant under a local $SU(2)$ transformation

$$F_i \rightarrow F_i W_i \quad (\text{A3})$$

where W is an $SU(2)$ matrix, this parton construction has an $SU(2)$ gauge redundancy.

Generically, a symmetry action on F_i is

$$F_i \rightarrow U_g(i)^\dagger F_{g(i)} G_g(i) \quad (\text{A4})$$

where i labels the site and g labels a symmetry action. Ref. [72] gives the expressions for U and G 's for $T_{1,2}$, C_6^* and σ^* :

$$\begin{aligned} U_{T_{1,2}} &= 1, \\ U_{C_6^*}(A) &= U_{C_6^*}(B) = \sigma_{C_6^*} \\ U_{\mathcal{T}\sigma^*}(A) &= U_{\mathcal{T}\sigma^*}(B) = \sigma_{\mathcal{T}\sigma^*} \end{aligned} \quad (\text{A5})$$

and

$$\begin{aligned} G_{T_{1,2}} &= 1 \\ G_{C_6^*}(A) &= -G_{C_6^*}(B) = \sigma_{C_6^*} \\ G_{\mathcal{T}\sigma^*}(A) &= G_{\mathcal{T}\sigma^*}(B) = \sigma_{\mathcal{T}\sigma^*} \end{aligned} \quad (\text{A6})$$

where A and B label the sublattice, and $\sigma_{C_6^*} \equiv \frac{1+i(\sigma_1+\sigma_2+\sigma_3)}{2}$ and $\sigma_{\mathcal{T}\sigma^*} \equiv e^{-i\sigma_3 \frac{\pi}{4}}$.

Because of the $SU(2)$ gauge redundancy (A3), it is equally valid to define another set of partons that are related to (A2) by a gauge transformation

$$\tilde{F}_i = \begin{pmatrix} \tilde{f}_{i1} & -\tilde{f}_{i2}^\dagger \\ \tilde{f}_{i2} & \tilde{f}_{i1}^\dagger \end{pmatrix} = F_i W_i \quad (\text{A7})$$

In terms of \tilde{F} , the symmetry actions become

$$\tilde{F}_i \rightarrow U_g(i)^\dagger \tilde{F}_{g(i)} \tilde{G}_g(i) \quad (\text{A8})$$

where

$$\tilde{G}_g(i) = W_{g(i)}^\dagger G_g(i) W_i \quad (\text{A9})$$

when g is unitary, or

$$\tilde{G}_g(i) = W_{g(i)}^\dagger G_g(i) W_i^* \quad (\text{A10})$$

when g is anti-unitary.

Now take W to be $W_{A(B)}$ on the $A(B)$ sublattice, with

$$\begin{aligned} W_A &= a + i(b\sigma_1 + a\sigma_3) \\ W_B &= e^{-i\sigma_3 \frac{\pi}{4}} W_A^* e^{i\sigma_3 \frac{\pi}{4}} \end{aligned} \quad (\text{A11})$$

where

$$a = \sqrt{\frac{1}{6 - 2\sqrt{3}}}, \quad b = (\sqrt{3} - 1)a \quad (\text{A12})$$

one can verify that

$$\begin{aligned} \tilde{G}_{T_{1,2}} &= 1 \\ \tilde{G}_{C_6^*}(A) &= \tilde{G}_{C_6^*}(B) = e^{i\sigma_3 \frac{5\pi}{6}} \\ \tilde{G}_{\mathcal{T}\sigma^*}(A) &= \tilde{G}_{\mathcal{T}\sigma^*}(B) = e^{-i\sigma_3 \frac{\pi}{4}} \end{aligned} \quad (\text{A13})$$

In terms of $\tilde{f}(\mathbf{r}_i) = \left(\tilde{f}_1(\mathbf{r}_i), \tilde{f}_2(\mathbf{r}_i) \right)^T$, the symmetry actions using \tilde{G}_i are

$$\begin{aligned} T_{1,2} : \tilde{f}(\mathbf{r}_i) &\rightarrow \tilde{f}(\mathbf{r}_i + \mathbf{n}_{1,2}) \\ C_6^* : \tilde{f}(\mathbf{r}_i) &\rightarrow e^{i\frac{5\pi}{6}} \sigma_{C_6^*}^\dagger \tilde{f}(C_6 \mathbf{r}_i) \\ \mathcal{T}\sigma^* : \tilde{f}(\mathbf{r}_i) &\rightarrow e^{-i\frac{\pi}{4}} \sigma_{\mathcal{T}\sigma^*}^\dagger \tilde{f}(\sigma \mathbf{r}_i) \end{aligned} \quad (\text{A14})$$

which is recorded in Table II.

B. Kitaev model in terms of $SU(2)$ partons

In this appendix we give the explicit expressions of (8).

First recall that at the mean field level the original Kitaev model described in [3] becomes a quadratic Hamiltonian of Majorana fermions $\chi_{A,B}^a$, with $a = 0, 1, 2, 3$ and $A(B)$ represents the sublattice index (we adopt the same notation as in Ref. [72]). It contains three types of terms:

$$H_K = H_1 + H_2 + H_3 \quad (\text{B1})$$

where H_1 is a nearest-neighbor coupling

$$H_1 = 2iJ_1 \sum_{\mathbf{r}_i} \left(\chi_B^0(\mathbf{r}_i) \chi_A^0(\mathbf{r}_i) + \chi_B^0(\mathbf{r}_i + \mathbf{n}_2) \chi_A^0(\mathbf{r}_i) + \chi_B^0(\mathbf{r}_i - \mathbf{n}_1) \chi_A^0(\mathbf{r}_i) \right), \quad (\text{B2})$$

H_2 is a next-nearest-neighbor coupling

$$\begin{aligned} H_2 = 2iJ_2 \sum_{\mathbf{r}_i} &\left(\chi_A^0(\mathbf{r}_i + \mathbf{n}_1) \chi_A^0(\mathbf{r}_i) + \chi_A^0(\mathbf{r}_i + \mathbf{n}_2) \chi_A^0(\mathbf{r}_i) + \chi_A^0(\mathbf{r}_i + \mathbf{n}_3) \chi_A^0(\mathbf{r}_i) \right. \\ &\left. - \chi_B^0(\mathbf{r}_i + \mathbf{n}_1) \chi_B^0(\mathbf{r}_i) - \chi_B^0(\mathbf{r}_i + \mathbf{n}_2) \chi_B^0(\mathbf{r}_i) - \chi_B^0(\mathbf{r}_i + \mathbf{n}_3) \chi_B^0(\mathbf{r}_i) \right) \end{aligned} \quad (\text{B3})$$

and H_3 is a nearest-neighbor coupling

$$H_3 = 2iJ'_1 \sum_{\mathbf{r}_i} \left(\chi_A^3(\mathbf{r}_i) \chi_B^3(\mathbf{r}_i) + \chi_A^1(\mathbf{r}_i - \mathbf{n}_2) \chi_B^1(\mathbf{r}_i) + \chi_A^2(\mathbf{r}_i + \mathbf{n}_1) \chi_B^2(\mathbf{r}_i) \right) \quad (\text{B4})$$

Notice for any values of J_1 , J_2 and J'_1 , this theory describes the same quantum phase (or the time reversal partner, depending on the sign of J_2) as in the Kitaev model. Since we are only concerned with universal properties, we will not worry the precise values of J_1 , J_2 and J'_1 .

In Ref. [72], the parton f in (6) or (A2) is related to the Majorana fermions via

$$f_1 = \frac{1}{\sqrt{2}} (\chi^0 + i\chi^3), \quad f_2 = \frac{1}{\sqrt{2}} (i\chi^1 - \chi^2) \quad (\text{B5})$$

We will instead relate these Majorana fermions to the transformed partons that is related to the above f 's via (A7), with the gauge transformation given by (A11). In terms of these partons, the Kitaev model (B1) can be written as (8).

Below we spell out the terms in (8). For notational simplicity, we will drop the tildes from now on, with the understanding that now we are using the transformed partons.

All terms in H_1 are of the form $2iJ_1\chi_B^0(\mathbf{r}_j)\chi_A^0(\mathbf{r}_i)$, which in terms of the transformed spinons reads

$$2iJ_1\chi_B^0(\mathbf{r}_j)\chi_A^0(\mathbf{r}_i) = J_1 \left\{ f_B^\dagger(\mathbf{r}_j) \left[\left(a^2 + \frac{b^2}{2} \right) + \left(a^2 - \frac{b^2}{2} \right) \sigma_3 + ab\sigma_1 + ab\sigma_2 \right] f_A(\mathbf{r}_i) + \text{h.c.} \right. \\ \left. + f_B^T(\mathbf{r}_j) \left[\left(ia^2 + \frac{b^2}{2} \right) + \left(ia^2 - \frac{b^2}{2} \right) \sigma_3 + ab(1+i)\sigma_1 \right] f_A(\mathbf{r}_i) + \text{h.c.} \right\} \quad (\text{B6})$$

where the first line goes into H_{hopping} , and the second line goes into H_{pairing} .

All terms in H_2 are of the form $2iJ_2\tau_z\chi^0(\mathbf{r}_j)\chi^0(\mathbf{r}_i)$, with $\tau_z = 1$ ($\tau_z = -1$) in the A (B) sublattice, which in terms of the transformed spinons reads

$$2iJ_2\tau_z\chi^0(\mathbf{r}_j)\chi^0(\mathbf{r}_i) = J_2 \left\{ f^\dagger(\mathbf{r}_j) \left[i \left(a^2 + \frac{b^2}{2} \right) + i \left(a^2 - \frac{b^2}{2} \right) \sigma_3 + iab\sigma_1 + iab\sigma_2 \right] \tau_z f(\mathbf{r}_i) + \text{h.c.} \right. \\ \left. + f^T(\mathbf{r}_j) \left[\left(a^2 - \frac{ib^2}{2} \right) + \left(a^2 + \frac{ib^2}{2} \right) \sigma_3 + ab(1-i)\sigma_1 \right] f(\mathbf{r}_i) + \text{h.c.} \right\} \quad (\text{B7})$$

Again, the first line goes into H_{hopping} and the second line goes into H_{pairing} .

The terms in H_3 depends on the type of the bond. The terms on the x -bonds (bonds along \mathbf{a}_1) are of the form $2iJ'_1\chi_A^1(\mathbf{r}_j)\chi_B^1(\mathbf{r}_i)$, which in terms of the transformed spinons reads

$$2iJ'_1\chi_A^1(\mathbf{r}_j)\chi_B^1(\mathbf{r}_i) = J'_1 \left\{ f_A^\dagger(\mathbf{r}_j) \left[\left(-a^2 - \frac{b^2}{2} \right) + \left(a^2 - \frac{b^2}{2} \right) \sigma_3 - ab\sigma_1 + ab\sigma_2 \right] f_B(\mathbf{r}_i) + \text{h.c.} \right. \\ \left. + f_A^T(\mathbf{r}_j) \left[\left(-ia^2 - \frac{b^2}{2} \right) - \left(-ia^2 + \frac{b^2}{2} \right) \sigma_3 - ab(1+i)\sigma_1 \right] f_B(\mathbf{r}_i) + \text{h.c.} \right\} \quad (\text{B8})$$

The terms on the y -bonds (bonds along \mathbf{a}_2) are of the form $2iJ'_1\chi_A^2(\mathbf{r}_j)\chi_B^2(\mathbf{r}_i)$, which in terms of the transformed spinons reads

$$2iJ'_1\chi_A^2(\mathbf{r}_j)\chi_B^2(\mathbf{r}_i) = J'_1 \left\{ f_A^\dagger(\mathbf{r}_j) \left[\left(-a^2 - \frac{b^2}{2} \right) + \left(a^2 - \frac{b^2}{2} \right) \sigma_3 + ab\sigma_1 - ab\sigma_2 \right] f_B(\mathbf{r}_i) + \text{h.c.} \right. \\ \left. + f_A^T(\mathbf{r}_j) \left[\left(ia^2 + \frac{b^2}{2} \right) + \left(-ia^2 + \frac{b^2}{2} \right) \sigma_3 - ab(1+i)\sigma_1 \right] f_B(\mathbf{r}_i) + \text{h.c.} \right\} \quad (\text{B9})$$

The terms on the z -bonds (bonds along \mathbf{a}_3) are of the form $2iJ'_1\chi_A^3(\mathbf{r}_j)\chi_B^3(\mathbf{r}_i)$, which in terms of the transformed spinons reads

$$2iJ'_1\chi_A^3(\mathbf{r}_j)\chi_B^3(\mathbf{r}_i) = J'_1 \left\{ f^\dagger(\mathbf{r}_j) \left[\left(-a^2 - \frac{b^2}{2} \right) - \left(a^2 - \frac{b^2}{2} \right) \sigma_3 + ab\sigma_1 + ab\sigma_2 \right] f(\mathbf{r}_i) + \text{h.c.} \right. \\ \left. + f^T(\mathbf{r}_j) \left[\left(-ia^2 - \frac{b^2}{2} \right) + \left(-ia^2 + \frac{b^2}{2} \right) \sigma_3 + ab(1+i)\sigma_1 \right] f(\mathbf{r}_i) + \text{h.c.} \right\} \quad (\text{B10})$$

The first lines in the right-hand-side always go into H_{hopping} , and the second lines always go into H_{pairing} .

C. Derivation of duality of critical theories

We can use the level-rank duality in Ref. [54] to show that the bosonic critical theory Eq. (15) is dual to the fermionic critical theory Eq. (18). We begin with a level-rank duality, namely, that the $U(2)_2$ theory with N_f fundamental bosons is dual to the $SU(2)_{-2+N_f/2}$ theory with N_f fundamental fermions. The duality only holds for $N_f = 1, 2$. The bosonic theory is,

$$\mathcal{L} = \sum_{I=1}^{N_f} |(\partial_\mu - i\mathbf{b}_\mu)\Phi_I|^2 - m \sum_I |\Phi_I|^2 - V(|\Phi|) - \frac{2}{4\pi} \text{Tr}(\mathbf{b}d\mathbf{b} - \frac{2i}{3}\mathbf{b}^3) - \frac{1}{2\pi} B'd(\text{Tr}\mathbf{b}). \quad (\text{C1})$$

And the fermionic dual is,

$$\mathcal{L} = \sum_{I=1}^{N_f} \bar{\Psi}_I (i\cancel{\partial} + \cancel{\phi} + \frac{B'}{2} \mathbf{1}_2 + m) \Psi_I + \frac{2 - N_f/2}{4\pi} \text{Tr} \left[\left(a + \frac{B'}{2} \mathbf{1}_2 \right) d \left(a + \frac{B'}{2} \mathbf{1}_2 \right) - \frac{2i}{3} \left(a + \frac{B'}{2} \mathbf{1}_2 \right)^3 \right] + (4 - N_f) \text{CS}_g, \quad (\text{C2})$$

Here \mathbf{b} is a $U(2)$ gauge field, a is a $SU(2)$ gauge field and B' is a $U(1)$ probe field. $V(\Phi)$ is the $SU(N_f)$ invariant quartic term.

Next we add a TQFT $U(1)_{-2}$ to both theories, yielding two new theories that are dual to each other. The bosonic theory changes to

$$\mathcal{L} = \sum_{I=1}^{N_f} |(\partial_\mu - i\mathbf{b}_\mu) \Phi_I|^2 - m \sum |\Phi_I|^2 - V(|\Phi|) - \frac{2}{4\pi} \text{Tr}(\mathbf{b} d\mathbf{b} - \frac{2i}{3} \mathbf{b}^3) - \frac{1}{2\pi} B' d(\text{Tr} \mathbf{b}) + \frac{2}{4\pi} \beta d\beta - \frac{1}{2\pi} \beta d(B - B'), \quad (\text{C3})$$

And the fermionic theory changes to,

$$\begin{aligned} \mathcal{L} = & \sum_{I=1}^{N_f} \bar{\Psi}_I (i\cancel{\partial} + \cancel{\phi} + \frac{B'}{2} \mathbf{1}_2 + m) \Psi_I + \frac{2 - N_f/2}{4\pi} \text{Tr} \left[\left(a + \frac{B'}{2} \mathbf{1}_2 \right) d \left(a + \frac{B'}{2} \mathbf{1}_2 \right) - \frac{2i}{3} \left(a + \frac{B'}{2} \mathbf{1}_2 \right)^3 \right] + (4 - N_f) \text{CS}_g \\ & + \frac{2}{4\pi} \beta d\beta - \frac{1}{2\pi} \beta d(B - B'). \end{aligned} \quad (\text{C4})$$

At last, we gauge the $U(1)$ probe field $B' \rightarrow \alpha$. In the bosonic theory, we can simply integrate out α , yielding $\beta = \text{Tr} \mathbf{b}$, and the theory exactly reduces to the bosonic critical theory Eq. (15) we introduced in the main text:

$$\mathcal{L} = \sum_{I=1}^{N_f} |(\partial_\mu - i\mathbf{b}_\mu) \Phi_I|^2 - m \sum |\Phi_I|^2 - V(|\Phi|) - \frac{2}{4\pi} \text{Tr}(\mathbf{b} d\mathbf{b} - \frac{2i}{3} \mathbf{b}^3) + \frac{2}{4\pi} (\text{Tr} \mathbf{b}) d(\text{Tr} \mathbf{b}) - \frac{1}{2\pi} B d(\text{Tr} \mathbf{b}), \quad (\text{C5})$$

In the fermionic theory, gauging B' will promote $a + \frac{B'}{2} \mathbf{1}_2$ to a $U(2)$ gauge field \mathbf{a} ,

$$\mathcal{L} = \sum_{I=1}^{N_f} \bar{\Psi}_I (i\cancel{\partial} + \cancel{\phi} + m) \Psi_I + \frac{2 - N_f/2}{4\pi} \text{Tr} \left[\mathbf{a} d\mathbf{a} - \frac{2i}{3} \mathbf{a}^3 \right] + (4 - N_f) \text{CS}_g + \frac{2}{4\pi} \beta d\beta - \frac{1}{2\pi} \beta d(B - (\text{Tr} \mathbf{a})). \quad (\text{C6})$$

This theory is exactly the fermionic critical theory Eq. (18) we introduced in the main text.

D. Parton mean field of the fermionic $U(2)$ critical theory

In this appendix, we discuss the parton mean-field ansatz for the ITO and its confinement transitions. As discussed in the main text, the $U(2)$ parton construction is $\tilde{S}^+ = \phi^\dagger f_a^\dagger f_b^\dagger$. There is a $U(2)$ gauge redundancy, and the (f_a, f_b) is the $U(2)$ fundamental. We further rewrite $\phi^\dagger = c_1^\dagger c_2^\dagger$. The mean field Hamiltonian of the fermionic partons (c, f) generally has the first, second and third nearest-neighbor hoppings, which should be consistent with the symmetries: translation symmetry, inversion C_2 and $\mathcal{T}\sigma^*$. We note that the symmetry actions of translation and inversion are simple on (c, f) , while the $\mathcal{T}\sigma^*$ symmetry transformation is implemented as,

$$\mathcal{T}\sigma^* : \quad i \rightarrow -i, \quad (\text{D1})$$

$$\tilde{S}_{\mathbf{r}}^{x,y} \rightarrow \tilde{S}_{\sigma\mathbf{r}}^{x,y}, \quad (\text{D2})$$

$$\tilde{S}_{\mathbf{r}}^z \rightarrow -\tilde{S}_{\sigma\mathbf{r}}^z, \quad (\text{D3})$$

$$c_{\mathbf{r}}^\dagger \rightarrow c_{\sigma\mathbf{r}}, \quad (\text{D4})$$

$$f_{\mathbf{r}}^\dagger \rightarrow f_{\sigma\mathbf{r}}. \quad (\text{D5})$$

The mean-field Hamiltonian for the partons (both c and f) takes a generic form with the first-, second- and third-nearest-neighbor hoppings, $H = -\sum_{ij} t_{ij} d_i^\dagger d_j$, where d can represent either f or c . Specifically, we consider a symmetry preserving hopping pattern, which has parameters $t_{1x} = t_{1y}$, t_{1z} , t_{2z} , $t_{3x} = t_{3y}$ and t_{3z} , as shown in Fig. 8.

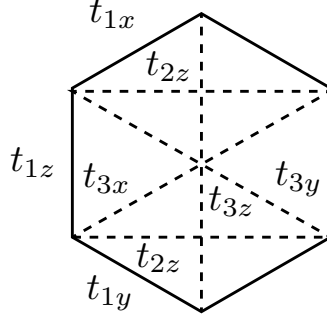


FIG. 8. The hopping terms of the parton mean-field ansatz.

	T_1	T_2	C_2	$\mathcal{T}\sigma^*$
$\bar{\Psi}\tau^x\Psi$	-1	-1	-1	1
$\bar{\Psi}\tau^y\Psi$	-1	-1	-1	-1
$\bar{\Psi}\tau^z\Psi$	1	1	1	-1
$\bar{\Psi}\gamma^0\Psi$	1	1	1	-1
$\bar{\Psi}\gamma^1\Psi$	1	1	-1	1
$\bar{\Psi}\gamma^2\Psi$	1	1	-1	-1
$\bar{\Psi}\gamma^0\tau^x\Psi$	-1	-1	-1	-1
$\bar{\Psi}\gamma^1\tau^x\Psi$	-1	-1	1	1
$\bar{\Psi}\gamma^2\tau^x\Psi$	-1	-1	1	-1
$\bar{\Psi}\gamma^0\tau^y\Psi$	-1	-1	-1	1
$\bar{\Psi}\gamma^1\tau^y\Psi$	-1	-1	1	-1
$\bar{\Psi}\gamma^2\tau^y\Psi$	-1	-1	1	1
$\bar{\Psi}\gamma^0\tau^z\Psi$	1	1	1	1
$\bar{\Psi}\gamma^1\tau^z\Psi$	1	1	-1	-1
$\bar{\Psi}\gamma^2\tau^z\Psi$	1	1	-1	1
\mathcal{M}_1	-1	-1	-1	$(-1)^s\mathcal{M}_2^\dagger$
\mathcal{M}_2	-1	-1	-1	$(-1)^s\mathcal{M}_1^\dagger$
\mathcal{M}_3	1	1	1	$-(-1)^s\mathcal{M}_3^\dagger$

TABLE IV. Symmetries of operators in the $N_f = 2$ critical theory with Dirac nodes at the M_1 and M_2 points. $s = 0, 1$ cannot be determined using our current method. There is one symmetry allowed relevant operator, $\bar{\Psi}\gamma^0\tau^z\Psi$, which will destroy the quantum critical point.

The parton $c_{1,2}$ is always in a $C = -1$ band, it corresponds to ϕ realizes $\nu = -1/2$ bosonic Laughlin state. Specifically we take the hopping amplitude as $t_{1x}^{c_1} = t_{1x}^{c_2} = 1$, $t_{1z}^{c_1} = 1$, $t_{2z}^{c_1} = 0.5e^{i\pi/2}$, and $t_{1x}^{c_2} = t_{1x}^{c_2} = 1$, $t_{1z}^{c_2} = -1$, $t_{2z}^{c_2} = 0.5e^{i\pi/2}$.

ITO is realized by putting $U(2)$ f -partons into a $C = 2$ band, which for example can be realized with hopping amplitude $t_{1x}^f = t_{1y}^f = 1$, $t_{1z}^f = 1$, $t_{2z}^f = 0.5e^{i\pi/2}$, $t_{3x}^f = t_{3y}^f = 0.3$, $t_{3z}^f = 1$. To realize the zigzag magnetic order, we need to tune the Chern number of f -partons to $C = 1$. It can be triggered by tuning $t_{1x}^f = t_{1y}^f$, and the transition happens at $t_{1x}^f = t_{1y}^f = 1.3$. Using this mean-field ansatz, we work out the symmetry quantum numbers of the relevant operators as summarized in Table I. We note that the quantum numbers of $d(\text{Tra})$ turn out to be identical to that of $\bar{\Psi}\gamma^\mu\Psi$ in all our fermionic dual theories, so they are not displayed in the tables.

To realize the transition from the ITO to the trivially polarized state, we need to tune the Chern number directly from $C = 2$ to $C = 0$. There are three different types of ways to realize this transition:

1. Tuning t_{1z}^f , and the transition happens at $t_{1z}^f = 1.6$. The two Dirac cones are at the M_1 and M_2 points.

	T_1	T_2	C_2	$\mathcal{T}\sigma^*$
$\bar{\Psi}_1\Psi_2$	e^{-2ik}	e^{-2ik}	$-\bar{\Psi}_2\Psi_1$	$-\bar{\Psi}_2\Psi_1$
$\bar{\Psi}_2\Psi_1$	e^{2ik}	e^{2ik}	$-\bar{\Psi}_1\Psi_2$	$-\bar{\Psi}_1\Psi_2$
$\bar{\Psi}\tau^z\Psi$	1	1	-1	1
$\bar{\Psi}\gamma^0\Psi$	1	1	1	-1
$\bar{\Psi}\gamma^1\Psi$	1	1	-1	1
$\bar{\Psi}\gamma^2\Psi$	1	1	-1	-1
$\bar{\Psi}_1\gamma^0\Psi_2$	e^{-2ik}	e^{-2ik}	$-\bar{\Psi}_2\gamma^0\Psi_1$	$\bar{\Psi}_2\gamma^0\Psi_1$
$\bar{\Psi}_1\gamma^1\Psi_2$	e^{-2ik}	e^{-2ik}	$\bar{\Psi}_2\gamma^1\Psi_1$	$-\bar{\Psi}_2\gamma^1\Psi_1$
$\bar{\Psi}_1\gamma^2\Psi_2$	e^{-2ik}	e^{-2ik}	$\bar{\Psi}_2\gamma^2\Psi_1$	$\bar{\Psi}_2\gamma^2\Psi_1$
$\bar{\Psi}_2\gamma^0\Psi_1$	e^{2ik}	e^{2ik}	$-\bar{\Psi}_1\gamma^0\Psi_2$	$\bar{\Psi}_1\gamma^0\Psi_2$
$\bar{\Psi}_2\gamma^1\Psi_1$	e^{2ik}	e^{2ik}	$\bar{\Psi}_1\gamma^1\Psi_2$	$-\bar{\Psi}_1\gamma^1\Psi_2$
$\bar{\Psi}_2\gamma^2\Psi_1$	e^{2ik}	e^{2ik}	$\bar{\Psi}_1\gamma^2\Psi_2$	$\bar{\Psi}_1\gamma^2\Psi_2$
$\bar{\Psi}\gamma^0\tau^z\Psi$	1	1	-1	-1
$\bar{\Psi}\gamma^1\tau^z\Psi$	1	1	1	1
$\bar{\Psi}\gamma^2\tau^z\Psi$	1	1	1	-1
\mathcal{M}_1	$-e^{2ik}$	$-e^{2ik}$	$-\mathcal{M}_2$	$(-1)^s\mathcal{M}_1^\dagger$
\mathcal{M}_2	$-e^{-2ik}$	$-e^{-2ik}$	$-\mathcal{M}_1$	$(-1)^s\mathcal{M}_2^\dagger$
\mathcal{M}_3	-1	-1	-1	$-(-1)^s\mathcal{M}_3^\dagger$

TABLE V. Symmetries of operators in the $N_f = 2$ critical theory with two Dirac cones on the high symmetry line $K - K'$. $s = 0, 1$ cannot be determined using our current method. There is one symmetry allowed relevant operator, $\bar{\Psi}\gamma^1\tau^z\Psi$, which however only moves the location of Dirac points without destroying the quantum critical point.

	T_1	T_2	C_2	$\mathcal{T}\sigma^*$
$\bar{\Psi}_1\Psi_2$	e^{-2ik}	e^{2ik}	$-\bar{\Psi}_2\Psi_1$	1
$\bar{\Psi}_2\Psi_1$	e^{2ik}	e^{-2ik}	$-\bar{\Psi}_1\Psi_2$	1
$\bar{\Psi}\tau^z\Psi$	1	1	-1	-1
$\bar{\Psi}\gamma^0\Psi$	1	1	1	-1
$\bar{\Psi}\gamma^1\Psi$	1	1	-1	1
$\bar{\Psi}\gamma^2\Psi$	1	1	-1	-1
$\bar{\Psi}_1\gamma^0\Psi_2$	e^{-2ik}	e^{2ik}	$-\bar{\Psi}_2\gamma^0\Psi_1$	-1
$\bar{\Psi}_1\gamma^1\Psi_2$	e^{-2ik}	e^{2ik}	$\bar{\Psi}_2\gamma^1\Psi_1$	1
$\bar{\Psi}_1\gamma^2\Psi_2$	e^{-2ik}	e^{2ik}	$\bar{\Psi}_2\gamma^2\Psi_1$	-1
$\bar{\Psi}_2\gamma^0\Psi_1$	e^{2ik}	e^{-2ik}	$-\bar{\Psi}_1\gamma^0\Psi_2$	-1
$\bar{\Psi}_2\gamma^1\Psi_1$	e^{2ik}	e^{-2ik}	$\bar{\Psi}_1\gamma^1\Psi_2$	1
$\bar{\Psi}_2\gamma^2\Psi_1$	e^{2ik}	e^{-2ik}	$\bar{\Psi}_1\gamma^2\Psi_2$	-1
$\bar{\Psi}\gamma^0\tau^z\Psi$	1	1	-1	1
$\bar{\Psi}\gamma^1\tau^z\Psi$	1	1	1	-1
$\bar{\Psi}\gamma^2\tau^z\Psi$	1	1	1	1
\mathcal{M}_1	$-e^{2ik}$	$-e^{-2ik}$	$-\mathcal{M}_2$	$-(-1)^s\mathcal{M}_2^\dagger$
\mathcal{M}_2	$-e^{-2ik}$	$-e^{2ik}$	$-\mathcal{M}_1$	$-(-1)^s\mathcal{M}_1^\dagger$
\mathcal{M}_3	-1	-1	-1	$(-1)^s\mathcal{M}_3^\dagger$

TABLE VI. Symmetries of operators in the $N_f = 2$ critical theory with two Dirac cones on the high symmetry line $M_3 - M_3$. $s = 0, 1$ cannot be determined using our current method. There is one symmetry allowed relevant operator, $\bar{\Psi}\gamma^2\tau^z\Psi$, which however only moves the location of Dirac points without destroying the quantum critical point.

In this case, the symmetry actions on Ψ are given by

$$\begin{aligned}
T_1 : \Psi &\rightarrow -\tau^z \Psi \\
T_2 : \Psi &\rightarrow \tau^z \Psi \\
C_2 : \Psi(\mathbf{r}) &\rightarrow \gamma^0 \tau^z \Psi(-\mathbf{r}) \\
\mathcal{T}\sigma^* : \Psi(x, y) &\rightarrow i\gamma^1 \tau^x \Psi^\dagger(x, -y)
\end{aligned} \tag{D6}$$

The quantum numbers of the gauge invariant relevant operators are summarized in Table IV.

2. Tuning $t_{3x}^f = t_{3y}^f$, and the transition happens at $t_{3x}^f = t_{3y}^f = 1$. The two Dirac cones are at $(k_1, k_2) = (k, k), (-k, -k)$, which are on the high symmetry line $K - K'$. In this case, the symmetry actions on Ψ are given by

$$\begin{aligned}
T_1 : \Psi &\rightarrow e^{ik\tau^z} \Psi \\
T_2 : \Psi &\rightarrow e^{ik\tau^z} \Psi \\
C_2 : \Psi(\mathbf{r}) &\rightarrow \gamma^0 \tau^y \Psi(-\mathbf{r}) \\
\mathcal{T}\sigma^* : \Psi(x, y) &\rightarrow i\gamma^1 \tau^z \Psi^\dagger(x, -y)
\end{aligned} \tag{D7}$$

The quantum numbers of the gauge invariant relevant operators are summarized in Table V.

3. Tuning t_{3z}^f , and the transition happens at $t_{3z}^f = 1.6$. The two Dirac cones are at $(k_1, k_2) = (k, -k), (-k, k)$, which are on the high symmetry line $M_3 - M_3$. In this case, the symmetry actions on Ψ are given by

$$\begin{aligned}
T_1 : \Psi &\rightarrow e^{ik\tau^z} \Psi \\
T_2 : \Psi &\rightarrow e^{-ik\tau^z} \Psi \\
C_2 : \Psi(\mathbf{r}) &\rightarrow \gamma^0 \tau^y \Psi(-\mathbf{r}) \\
\mathcal{T}\sigma^* : \Psi(x, y) &\rightarrow i\gamma^1 \tau^x \Psi^\dagger(x, -y)
\end{aligned} \tag{D8}$$

The quantum numbers of the gauge invariant relevant operators are summarized in Table VI.

At last, we make a few comments on the monopole operators. Technically, we follow the method in Ref. [74, 103, 104] to calculate the quantum numbers of the monopoles. Namely, we explicitly construct the monopole states on a torus, and then extract the quantum number of the monopole states. Specifically, we put the system on a $2 \times L \times L$ lattice, and spread a uniform 2π flux for each parton c, f . Each Dirac fermion will form Landau levels with one exact zero mode. When $N_f = 1$, the gauge invariant monopole corresponds to a state with all negative-energy Fermi sea filled. In contrast, in the $N_f = 2$ critical theory, the gauge invariant monopoles should have two zero modes filled (each from one $U(2)$ color) together with the filled negative-energy Fermi sea. There are three gauge invariant ways to fill the zero modes,

$$\mathcal{M}_1 = \widetilde{\mathcal{M}}\psi_{1a}\psi_{1b}, \quad \mathcal{M}_2 = \widetilde{\mathcal{M}}\psi_{2b}\psi_{2a}, \quad \mathcal{M}_3 = \frac{1}{\sqrt{2}}\widetilde{\mathcal{M}}(\psi_{1a}\psi_{2b} - \psi_{1b}\psi_{2a}). \tag{D9}$$

Here $\widetilde{\mathcal{M}}$ is the bare monopole with 2π flux and filled negative-energy Fermi sea. ψ represents the zero mode, and 1, 2 are the flavor indices and a, b are the color indices. The three monopoles are in the adjoint representation of the $SU(2)$ flavor symmetry. Using our current method, we are not able to determine the quantum number of the monopoles under $\mathcal{T}\sigma^*$, for which there is an undetermined sign $\mathcal{M} \rightarrow \pm\mathcal{M}^\dagger$. In the $N_f = 1$ theory, we speculate the sign is -1 , hence it matches the quantum number of the zigzag order. In the $N_f = 2$ theory, we leave this sign undetermined, and it has no influence on our discussion on the nature of the confined state.

More details on the quantum numbers of monopoles

Before finishing this appendix, we discuss in more details the symmetry actions on the monopoles of the fermionic critical theory with $N_f = 2$, using state-operator correspondence. Including both colors and spins, there will be four zero modes in the presence of $\pm 2\pi$ background flux. In this case there is no Chern-Simons term

for $\text{Tr}(\mathbf{a})$, so two of the zero modes need to be occupied to form a gauge invariant state (operator). In terms of states, there are three different ways to occupy these zero modes and make a color singlet:

$$f_{1a}^\dagger f_{1b}^\dagger |0\rangle, \quad f_{2b}^\dagger f_{2a}^\dagger |0\rangle, \quad \frac{1}{\sqrt{2}}(f_{1a}^\dagger f_{2b}^\dagger - f_{1b}^\dagger f_{2a}^\dagger) |0\rangle \quad (\text{D10})$$

where the f 's are the operators of the zero modes, and $|0\rangle$ is the ground state under a 2π background flux with no zero mode occupied. We use 1 and 2 to label the two different flavors, and a and b to label the two different colors. These states correspond to the operators $\mathcal{M}_{1,2,3}$ in Eq (D9), respectively.

The actions of $T_{1,2}$ and C_2 are simpler because they do not take the monopole operators to their hermitian conjugates. To determine the action of $\mathcal{T}\sigma^*$, which takes the monopoles to their hermitian conjugates, it will be important to first identify the corresponding states of the hermitian conjugates of these operators. This can be worked out using the methods in Refs. [78, 79]. More precisely, let us write the three states in Eq. (D10) in a more suggestive form

$$\begin{aligned} \mathcal{M}_1 &\sim f_{1a}^\dagger f_{1b}^\dagger |0\rangle = \left(f^T \frac{(1 + \tau^z)\epsilon}{4} f \right)^* |0\rangle = \left(f^T \tau^y \frac{(\tau^y + i\tau^x)}{4} f \right)^* |0\rangle \\ \mathcal{M}_2 &\sim f_{2b}^\dagger f_{1a}^\dagger |0\rangle = \left(-f^T \frac{(1 - \tau^z)\epsilon}{4} f \right)^* |0\rangle = \left(-f^T \tau^y \frac{(\tau^y - i\tau^x)\epsilon}{4} f \right)^* |0\rangle \\ \mathcal{M}_3 &\sim \frac{1}{\sqrt{2}}(f_{1a}^\dagger f_{2b}^\dagger - f_{1b}^\dagger f_{2a}^\dagger) |0\rangle = \frac{1}{\sqrt{2}} \left(f^T \frac{\tau^x \epsilon}{4} f \right)^* |0\rangle = \frac{1}{\sqrt{2}} \left(f^T \tau^y \frac{-i\tau^z \epsilon}{4} f \right)^* |0\rangle \end{aligned} \quad (\text{D11})$$

where τ acts on the flavor space and ϵ acts on the color space. From these we get

$$\begin{aligned} i(\mathcal{M}_1 + \mathcal{M}_2) &\sim \left(f^T \tau^y \tau^x \frac{\epsilon}{2} f \right)^* |0\rangle \\ \mathcal{M}_1 - \mathcal{M}_2 &\sim \left(f^T \tau^y \tau^y \frac{\epsilon}{2} f \right)^* |0\rangle \\ -2i\mathcal{M}_3 &\sim \frac{1}{\sqrt{2}} \left(f^T \tau^y \frac{\tau^z \epsilon}{2} f \right)^* |0\rangle \end{aligned} \quad (\text{D12})$$

Therefore, $(\mathcal{M}_1 - \mathcal{M}_2, i(\mathcal{M}_1 + \mathcal{M}_2), -2i\mathcal{M}_3)$ transforms as a vector under the $SU(2)$ flavor symmetry. Because this representation of the $SU(2)$ transformation is real, $(\mathcal{M}_1^\dagger - \mathcal{M}_2^\dagger, -i(\mathcal{M}_1^\dagger + \mathcal{M}_2^\dagger), 2i\mathcal{M}_3^\dagger)$ also transforms in the same representation under the $SU(2)$ flavor symmetry. This observation tells us what the corresponding states of these hermitian conjugates are (up to an undetermined phase factor):

$$\begin{aligned} -i(\mathcal{M}_1^\dagger + \mathcal{M}_2^\dagger) &\sim \left(\tilde{f}^T \tau^y \tau^x \frac{\epsilon}{2} \tilde{f} \right)^* |\tilde{0}\rangle \\ \mathcal{M}_1^\dagger - \mathcal{M}_2^\dagger &\sim \left(\tilde{f}^T \tau^y \tau^y \frac{\epsilon}{2} \tilde{f} \right)^* |\tilde{0}\rangle \\ 2i\mathcal{M}_3^\dagger &\sim \frac{1}{\sqrt{2}} \left(\tilde{f}^T \tau^y \frac{\tau^z \epsilon}{2} \tilde{f} \right)^* |\tilde{0}\rangle \end{aligned} \quad (\text{D13})$$

where $|\tilde{0}\rangle$ is the ground state under a -2π background flux with no zero modes occupied, and \tilde{f} 's are the corresponding zero modes under a -2π flux background. From the above we get

$$\begin{aligned} \mathcal{M}_1^\dagger &\sim -\tilde{f}_{2b}^\dagger \tilde{f}_{2a}^\dagger |\tilde{0}\rangle \\ \mathcal{M}_2^\dagger &\sim -\tilde{f}_{1a}^\dagger \tilde{f}_{1b}^\dagger |\tilde{0}\rangle \\ \mathcal{M}_3^\dagger &\sim -\frac{1}{\sqrt{2}} \left(\tilde{f}_{1a}^\dagger \tilde{f}_{2b}^\dagger - \tilde{f}_{1b}^\dagger \tilde{f}_{2a}^\dagger \right) |\tilde{0}\rangle \end{aligned} \quad (\text{D14})$$

Now we can check the action of $\mathcal{T}\sigma^*$ on $\mathcal{M}_{1,2,3}$. We have two types of actions of $\mathcal{T}\sigma^*$ on the fermions. For the first type:

$$\mathcal{T}\sigma^* : \Psi(x, y) \rightarrow i\gamma^1 \tau^x \Psi(x, -y)^\dagger \quad (\text{D15})$$

we have

$$\begin{aligned}
\mathcal{M}_1 &\sim f_{1a}^\dagger f_{1b}^\dagger |0\rangle \rightarrow \tilde{f}_{2a} \tilde{f}_{2b} \tilde{f}_{1a}^\dagger \tilde{f}_{1b}^\dagger \tilde{f}_{2a}^\dagger \tilde{f}_{2b}^\dagger |\tilde{0}\rangle = -\tilde{f}_{1a}^\dagger \tilde{f}_{1b}^\dagger |\tilde{0}\rangle \sim \mathcal{M}_2^\dagger \\
\mathcal{M}_2 &\sim f_{2b}^\dagger f_{2a}^\dagger |0\rangle \rightarrow \tilde{f}_{1b} \tilde{f}_{1a} \tilde{f}_{1a}^\dagger \tilde{f}_{1b}^\dagger \tilde{f}_{2a}^\dagger \tilde{f}_{2b}^\dagger |\tilde{0}\rangle = \tilde{f}_{2a}^\dagger \tilde{f}_{2b}^\dagger |\tilde{0}\rangle \sim \mathcal{M}_1^\dagger \\
\mathcal{M}_3 &\sim \frac{1}{\sqrt{2}} \left(f_{1a}^\dagger f_{2b}^\dagger - f_{1b}^\dagger f_{2a}^\dagger \right) |0\rangle \rightarrow \frac{1}{\sqrt{2}} \left(\tilde{f}_{2a} \tilde{f}_{1b} - \tilde{f}_{2b} \tilde{f}_{1a} \right) \tilde{f}_{1a}^\dagger \tilde{f}_{1b}^\dagger \tilde{f}_{2a}^\dagger \tilde{f}_{2b}^\dagger |\tilde{0}\rangle \\
&= \frac{1}{\sqrt{2}} \left(\tilde{f}_{1a}^\dagger \tilde{f}_{2b}^\dagger - \tilde{f}_{1b}^\dagger \tilde{f}_{2a}^\dagger \right) |\tilde{0}\rangle \sim -\mathcal{M}_3^\dagger
\end{aligned} \tag{D16}$$

In the above we have taken the convention that, under $\mathcal{T}\sigma^*$, $|0\rangle \rightarrow \tilde{f}_{1a}^\dagger \tilde{f}_{1b}^\dagger \tilde{f}_{2a}^\dagger \tilde{f}_{2b}^\dagger |\tilde{0}\rangle$. Notice these transformation rules have a common undetermined phase factor for $\mathcal{M}_{1,2,3}$.

For the second type of $\mathcal{T}\sigma^*$:

$$\mathcal{T}\sigma^* : \Psi(x, y) \rightarrow i\gamma^1 \tau^z \Psi(x, -y)^\dagger \tag{D17}$$

we have

$$\begin{aligned}
\mathcal{M}_1 &\sim f_{1a}^\dagger f_{1b}^\dagger |0\rangle \rightarrow \tilde{f}_{1a} \tilde{f}_{1b} \tilde{f}_{1a}^\dagger \tilde{f}_{1b}^\dagger \tilde{f}_{2a}^\dagger \tilde{f}_{2b}^\dagger |\tilde{0}\rangle = -\tilde{f}_{2a}^\dagger \tilde{f}_{2b}^\dagger |\tilde{0}\rangle \sim -\mathcal{M}_1^\dagger \\
\mathcal{M}_2 &\sim f_{2b}^\dagger f_{2a}^\dagger |0\rangle \rightarrow \tilde{f}_{2b} \tilde{f}_{2a} \tilde{f}_{1a}^\dagger \tilde{f}_{1b}^\dagger \tilde{f}_{2a}^\dagger \tilde{f}_{2b}^\dagger |\tilde{0}\rangle = \tilde{f}_{1a}^\dagger \tilde{f}_{1b}^\dagger |\tilde{0}\rangle \sim -\mathcal{M}_2^\dagger \\
\mathcal{M}_3 &\sim \frac{1}{\sqrt{2}} \left(f_{1a}^\dagger f_{2b}^\dagger - f_{1b}^\dagger f_{2a}^\dagger \right) |0\rangle \rightarrow \frac{1}{\sqrt{2}} \left(-\tilde{f}_{1a} \tilde{f}_{2b} + \tilde{f}_{1b} \tilde{f}_{2a} \right) \tilde{f}_{1a}^\dagger \tilde{f}_{1b}^\dagger \tilde{f}_{2a}^\dagger \tilde{f}_{2b}^\dagger |\tilde{0}\rangle \\
&= \frac{1}{\sqrt{2}} \left(\tilde{f}_{1b} \tilde{f}_{2a} - \tilde{f}_{1a} \tilde{f}_{2b} \right) |\tilde{0}\rangle \sim \mathcal{M}_3^\dagger
\end{aligned} \tag{D18}$$

Again, there is a common undetermined phase factor for the transformation rules of $\mathcal{M}_{1,2,3}$.

To summarize, this discussion tells us about the action of $\mathcal{T}\sigma^*$ on the monopole operators in the fermionic critical theory with $N_f = 2$. Similar arguments can establish the actions of other symmetries on these monopoles. However, this method leaves an undetermined common phase factor in each transformation of $\mathcal{M}_{1,2,3}$. For unitary symmetries $T_{1,2}$ and C_2 , we determine this phase factor numerically. For the anti-unitary symmetry $\mathcal{T}\sigma^*$, the current numerical method is insufficient to pin down this phase factor, and we leave it open. The results are listed in Tables IV V and VI. Notice for the fermionic critical theory with $N_f = 2$, the quantum numbers of monopoles will not affect the nature of the confined phase at all. Furthermore, in the cases with the Dirac points located at two generic momenta on the $K - K'$ line or the $M_3 - M_3$ line, where no symmetry allowed fermion bilinear perturbation can destroy the critical point, the unitary symmetries already forbid single monopole operators, while two-fold monopole operators are always symmetry allowed, regardless of what the undetermined phase factors in the actions of $\mathcal{T}\sigma^*$ are.